Z. Angew. Math. Phys. (2017) 68:95

0044-2275/17/040001-32
published online August 5, 2017
DOI 10.1007/s00033-017-0842-4

Zeitschrift für angewandte Mathematik und Physik ZAMP

An accurate and efficient analytical method for 1D hexagonal quasicrystal coating based on Green's function

Peng-Fei Hou, Bing-Jie Chen and Yang Zhang

Abstract. As a solid material between the crystal and the amorphous, the study on quasicrystals has become an important branch of condensed matter physics. Due to the special arrangement of atoms, quasicrystals own some desirable properties, such as low friction coefficient, low adhesion, high wear resistance and low porosity. Thus, quasicrystals are expected to be applied to the coating surfaces for engines, solar cells, nuclear fuel containers and heat converters. However, when the quasicrystals are used as coating material, it is very hard to simulate the coupling fields by the finite elements numerical methods because of its thin thickness and extreme stress gradient. This is the main reason why the structure of quasicrystal coating cannot be calculated accurately and stably by various numerical platform. A general solution method which can be used to solve this contact problem for a 1D hexagonal quasicrystal coating perfectly bonded to a transversely isotropic semi-infinite substrate under the point force is presented in this paper. The solutions of the Green's function under the distributed load can be obtained through the superposition principle. The simulation results show that this method is correct and effective, which has high calculation accuracy and fast convergence speed. The phonon–phason coupling field and elastic field in the coating and semi-infinite substrate will be derived based on the axisymmetric general solution, and the complicated coupling field of quasicrystals in coating contact space is explicitly presented in terms of elementary functions. In addition, the relationship between the coating thickness or external force and the stress component is also obtained to solve practical problems in engineering applications. The solutions presented not only bear theoretical merits, but also can serve as benchmarks to clarify various approximate methods.

Mathematics Subject Classification. 65-02 Research exposition (monographs, survey articles).

Keywords. 1D hexagonal quasicrystals, Coating contact, 3D Green's function, Phonon–phason coupling field, Isotropic material, Transversely isotropic material, Distributed forces.

1. Introduction

Since Shechtman [1] discovered the icosahedral quasicrystals (QCs) in Al–Mn alloys around 1984, the structures and properties of quasicrystals had been intensively investigated in experimental and theoretical analysis [2]. Quasicrystals are such solid materials which do not have the lattice with periodic orderly arrangement, but show long-range order [1]. The quasiperiodic symmetry structure presents great theoretical significance. Numerous quasicrystals materials with stable property were produced; it will be a new structure material and owns applied prospects. Now, the study of quasicrystals has become an important branch of condensed matter physics [2].

Quasicrystals not only have high academic research value, but also have potential engineering application prospect. The research of quasicrystals is the supplement and development about traditional crystallography. It has opened up a new field in mineral crystal structure research, which is of great significance in solid-state physics and material science. Quasicrystal materials have unique physical, mechanical and chemical properties. Due to the special arrangement of atoms, quasicrystals have some desirable properties, such as low friction coefficient, low adhesion, high wear resistance and low porosity. Thus, quasicrystals are expected to be used as coating surfaces for engines, solar cells, nuclear fuel containers and heat converters. Because of the special optical properties and sufficient thermal stability, quasicrystals are also used as the thin materials of solar energy industrial.

1.1. The properties of quasicrystals

With the framework of Landau theory, the elastic energy of quasicrystals was formulated by Bak et al. [3]. Unlike the normal crystals, there are a phonon field and a phason field simultaneously acting on the quasicrystals, as discussed by Bak [3,4]. These two mechanical variables have completely different properties. The phonon field displacement describes the grid wave which caused by the small vibrations when the atom deviates from the equilibrium position. The quantum of this grid wave is the phonon. The excitation of low-energy long wave element is the propagation-type. The phason field displacements describe the re-arrangement of quasiperiodic structures, resulting in another type of excitation of low-energy long wave element, which is diffusion-type and causes local energy perturbations. However, this is not two independent systems, the phonon and phason field influence each other. Therefore, the constitutive relation of the quasicrystals will include the phonon elastic constant, the phason elastic constant and the phonon–phason coupling constant. Quasicrystals own complex structure and belong to new emerging materials, so these constants are not fully accurate. By means of neutron diffraction and X-ray diffraction, Letoublon et al. [5–7] measured the elastic constants of some icosahedral quasicrystals. The independent elastic constants of the two-dimensional tenfold symmetric quasicrystal Al–Ni–Co are obtained in the literature [8,9]. Particularly, the cooperation coefficient about the phonon–phason coupling field interacting with the common elastic field still needs further theoretical research. Other physical properties of quasicrystals, especially the linear elasticity theory, have been widely investigated [10–15].

1.2. The classification of quasicrystals

Quasicrystals are divided into 1D quasicrystals, 2D quasicrystals and 3D quasicrystals, according to the arrangement of quasicrystal atoms. The atoms of 1D quasicrystals are arranged in quasiperiodic order on the symmetry axis and periodically on the plane perpendicular to the symmetry axis. The atomic structure of 2D quasicrystals is arranged in a periodic arrangement in the direction of the symmetry axis and quasiperiod in a plane perpendicular to the axis. The atomic structure of 3D quasicrystals is quasiperiodic arranged in the whole 3D space.

1.3. The Green's function of quasicrystals

In the study of quasicrystal Green's functions, the fundamental solutions are based on the relevant general solutions. The general solution of quasicrystals has also experienced a lot of scientific inquiry. Dimensional problems, three-dimensional problems, dynamic problems and thermoelastic problems [16–20] have been proposed. In addition, the general solutions of multidimensional quasicrystals are obtained [21–24] at the same time. With the improvement of quasicrystal general solution, the application of Green's function in solid mechanics becomes more and more mature. Based on De et al. [25] and Bachteler et al. [26], Chen et al. [19] proposed a general solution to the 1D hexagonal quasicrystals elasticity equation. After that, Wang [20] proposed a set of operator theory to solve the 1D hexagonal quasicrystals dynamical problem, but this theory only meets the higher-order partial differential function, so it cannot be widely used. Finally, Gao et al. [27] used the method of decomposition and superposition and developed a set of solutions to meet the general quasiharmonic function. In 2013, Li et al. [28,29] studied the problem of 1D hexagonal quasicrystals infinite body acted by point heat source and obtained the two-dimensional Green 's function solutions. In 2014, Li et al. [30,31] deduced the fundamental solutions of 1D hexagonal quasicrystals about piezoelectric effect and inferred the general solutions about thermo-electroelasticity as well as the fundamental solutions in infinite and semi-infinite bodies. Gao et al. [32] studied the problem of 2D quasicrystal infinite body under the action of concentrated force. On the basis of the 2D hexagonal quasicrystal general solution, Wang et al. [33] solved the fundamental solution of the three-dimensional

statics under concentrated force. Markus et al. [34] have recently done some research about the generalized elasticity and dislocation theory. These studies have played an important role in solving problems such as crack, contact and interlayer.

1.4. Research methods of coating materials

At present, the quantitative analysis method of coating structure can be divided into numerical method and analytic method. Numerical method mainly includes finite element method (FEM) [35–37] and boundary element method (BEM) [38,39]. The analytical method includes integral transformation method, transfer matrix method and classical general solution method. Finite element method and boundary element method are widely used in the field of solid mechanics to solve singular, infinite domain and semi-infinite domain problems, because they have the advantages of clear structure and high precision. However, both the finite element method and the boundary element method face the same problem when dealing with coating problems. Because the coating material is extremely thin relative to the attached substrate. When using finite element method, it will inevitably lead to unit distortion due to the very small coating mesh, resulting in the increase in calculation and calculation error. If the boundary element method is used, nearly singular integrals are generated when the coating boundary is calculated, which increases the difficulty of calculation.

Integral transformation method is a common method in solving differential equations. Through a series of integral transformation, the number of the original partial differential equations' independent variables continue to reduce and the ordinary differential equation could be obtained which is used to obtain the algebraic equation. When dealing with the layered structure by integral transformation method, the integral variable of each layer can be obtained directly through the whole system [40,41], or by constructing the stiffness matrix and the flexibility matrix. But with the increase in the number of layers, the whole structure matrix will become large and not conducive to the calculation. In contrast to the integral transformation method, transfer matrix method [42–44] is usually used to calculate the transfer matrix under fourth order because of its extensive calculation, although the linked matrix can be established between layers to achieve the matrix integration. With the increase in the order of the transfer matrix, the difficulty of the transfer matrix calculation is doubled, which brings great difficulties to the calculation of 3D multi-field coupling problems.

The general solution theory [45–51] is a classical method of mechanics, which solves the general solution of the partial differential equation directly through the control equation of the mechanical model and then obtains the special solution according to the boundary condition of the concrete problem. Finally, the corresponding solution is obtained by superposing the special solution and the general solution. The general solution theory can solve the mechanical calculation problem of any multilayer structure and has high accuracy. The general solution is usually composed of a harmonic function and one or more higher-order functions, but there is no standard to choose the harmonic function, only by experience accumulation and certain skills. So the application of general solution has its limitations.

1.5. The research emphasis of this paper

In this paper, the analytical solution of 1D hexagonal quasicrystals is derived. Not only the Green 's function solutions of 1D hexagonal quasicrystals in complete contact with transversely isotropic materials are given, the relationships between the elastic field and the coating thickness as well as the external forces are also obtained, when the quasicrystal is used as the coating material and acted by different kinds of loads at the same time. The general solution of 1D hexagonal quasicrystals is derived based on the general solution of transversely isotropic piezoelectric materials proposed by Ding et al. [52]. The corresponding Green's functions are derived by superposition principle and boundary condition of contact region. The

potential equation theory is used to solve the integral equation, and the three-dimensional general solution of the contact problem is obtained.

The Green's function in this paper is the analytic solution of the whole field under the unit concentrated force. In order to obtain the solution under different distributed forces (cone force, cylindrical force, uniform force, ellipsoid force, etc.), the matrix of the Green's function solution should be superimposed appropriately. The analytical solution, without any increase in the calculation amount, will be obtained through the combination of MATLAB programming skills and the Green's function matrix. This method can be used to simulate the solutions of quasicrystals quickly when working in different conditions. Which provides a detailed theoretical basis for the industrial application of 1D hexagonal quasicrystals.

2. General solutions for 1D hexagonal quasicrystals and transversely isotropic material

2.1. General solutions for 1D hexagonal quasicrystals

Considering 1D hexagonal quasicrystals whose atoms are arranged periodically in the $rO\phi$ plane and quasiperiodically in the z-direction in cylindrical coordinates (r, ϕ, z), according to Chen et al. [19] and Wang et al. [53], the constitutive laws of quasicrystals are

$$\begin{aligned}
\sigma_r &= c_{11}\frac{\partial u_r}{\partial r} + c_{12}\left(\frac{u_r}{r} + \frac{1}{r}\frac{\partial u_\phi}{\partial \phi}\right) + c_{13}\frac{\partial u_z}{\partial z} + R_1\frac{\partial w}{\partial z},\\
\sigma_\phi &= c_{12}\frac{\partial u_r}{\partial r} + c_{11}\left(\frac{u_r}{r} + \frac{1}{r}\frac{\partial u_\phi}{\partial \phi}\right) + c_{13}\frac{\partial u_z}{\partial z} + R_1\frac{\partial w}{\partial z},\\
\sigma_z &= c_{13}\left(\frac{\partial u_r}{\partial r} + \frac{u_r}{r} + \frac{1}{r}\frac{\partial u_\phi}{\partial \phi}\right) + c_{33}\frac{\partial u_z}{\partial z} + R_2\frac{\partial w}{\partial z},\\
\tau_{\phi z} &= c_{44}\left(\frac{\partial u_\phi}{\partial z} + \frac{1}{r}\frac{\partial u_z}{\partial \phi}\right) + R_3\frac{1}{r}\frac{\partial w}{\partial \phi},\\
\tau_{zr} &= c_{44}\left(\frac{\partial u_z}{\partial r} + \frac{\partial u_r}{\partial z}\right) + R_3\frac{\partial w}{\partial r},\\
\tau_{r\phi} &= c_{66}\left(\frac{1}{r}\frac{\partial u_r}{\partial \phi} + \frac{\partial u_\phi}{\partial r} - \frac{u_\phi}{r}\right),\\
H_r &= R_3\left(\frac{\partial u_z}{\partial r} + \frac{\partial u_r}{\partial z}\right) + K_2\frac{\partial w}{\partial r},\\
H_\phi &= R_3\left(\frac{\partial u_\phi}{\partial z} + \frac{1}{r}\frac{\partial u_z}{\partial \phi}\right) + K_2\frac{1}{r}\frac{\partial w}{\partial \phi},\\
H_z &= R_1\left(\frac{\partial u_r}{\partial r} + \frac{u_r}{r} + \frac{1}{r}\frac{\partial u_\phi}{\partial \phi}\right) + R_2\frac{\partial u_z}{\partial z} + K_1\frac{\partial w}{\partial z},
\end{aligned} \tag{1}$$

where $u_m\,(m = r, \phi, z)$ and w are the strain components expressed in terms of the phonon displacements and phason ones; σ_m, τ_{mn} are the components of stress in the phonon fields and $H_m(m, n = r, \phi, z)$ are the stress components in the phason fields; c_{ij}, R_{ij} and K_{ij} represent the phonon, phason and phonon–phason coupling elastic constants, respectively. The relation $c_{66} = (c_{11} - c_{12})/2$ holds for 1D hexagonal quasicrystals with transverse isotropy.

Ignoring the effects of body force, the generalized equilibrium equations for 1D hexagonal quasicrystals are:

$$\begin{aligned}
&\frac{\partial \sigma_r}{\partial r}+\frac{1}{r}\frac{\partial \tau_{r\phi}}{\partial \phi}+\frac{\partial \tau_{zr}}{\partial z}+\frac{\sigma_r-\sigma_\phi}{r}=0,\\
&\frac{\partial \tau_{r\phi}}{\partial r}+\frac{1}{r}\frac{\partial \sigma_\phi}{\partial \phi}+\frac{\partial \tau_{\phi z}}{\partial z}+\frac{2\tau_{r\phi}}{r}=0,\\
&\frac{\partial \tau_{zr}}{\partial r}+\frac{1}{r}\frac{\partial \tau_{\phi z}}{\partial \phi}+\frac{\partial \sigma_z}{\partial z}+\frac{\tau_{zr}}{r}=0,\\
&\frac{1}{r}\frac{\partial}{\partial r}\left(rH_r\right)+\frac{1}{r}\frac{\partial H_\phi}{\partial \phi}+\frac{\partial H_z}{\partial z}=0.
\end{aligned} \tag{2}$$

Taking the similarities between 1D hexagonal quasicrystals and transversely isotropic piezoelectric material into account, the general solution for governing Eqs. (1, 2) could be substituted equivalently for that presented by Ding et al. [52]. As for axisymmetric problem, the corresponding general solution is in the following form:

$$u_r=\sum_{j=1}^{3}\frac{\partial \psi_j}{\partial r},\quad u_z=\sum_{j=1}^{3}s_jk_{1j}\frac{\partial \psi_j}{\partial z_j},\quad w=\sum_{j=1}^{3}s_jk_{2j}\frac{\partial \psi_j}{\partial z_j}, \tag{3a}$$

$$\begin{aligned}
\sigma_r&=-2c_{66}\sum_{j=1}^{3}\frac{1}{r}\frac{\partial \psi_j}{\partial r}-\sum_{j=1}^{3}s_j^2\omega_{1j}\frac{\partial^2\psi_j}{\partial z_j^2},\\
\sigma_\phi&=2c_{66}\sum_{j=1}^{3}\frac{1}{r}\frac{\partial \psi_j}{\partial r}\ -\sum_{j=1}^{3}\left(s_j^2\omega_{1j}-2c_{66}\right)\frac{\partial^2\psi_j}{\partial z_j^2},\\
\sigma_z&=\sum_{j=1}^{3}\omega_{1j}\frac{\partial^2\psi_j}{\partial z_j^2},\quad \tau_{zr}=\sum_{j=1}^{3}s_j\omega_{1j}\frac{\partial^2\psi_j}{\partial r\partial z_j},\\
H_r&=\sum_{j=1}^{3}s_j\omega_{2j}\frac{\partial^2\psi_j}{\partial r\partial z_j},\quad H_z=\sum_{j=1}^{3}\omega_{2j}\frac{\partial^2\psi_j}{\partial z_j^2},
\end{aligned} \tag{3b}$$

where $\psi_j\,(j=1,2,3)$ are functions which satisfy following quasiharmonic equations:

$$\left(\frac{\partial^2}{\partial r^2}+\frac{\partial}{r\partial r}+\frac{\partial^2}{\partial z_j^2}\right)\psi_j=0\quad (j=1,2,3), \tag{4}$$

and

$$z_j=s_jz,(j=1,2,3). \tag{5}$$

$s_j\,(j=1,2,3)$, which satisfy $\mathrm{Re}(s_j)>0$, are three eigenvalues of following algebraic equation of the sixth orders:

$$a_0s^6-b_0s^4+d_0s^2-f_0=0, \tag{6}$$

where

$$\begin{aligned}
a_0&=c_{44}\left(R_2^2-c_{33}K_1\right),\\
b_0&=c_{33}\left[-c_{44}K_2+\left(R_1+R_3\right)^2\right]-K_1\left[c_{11}c_{33}+c_{44}^2-\left(c_{13}+c_{44}\right)^2\right]\\
&\quad+R_2\left[2c_{44}R_3+c_{11}R_2-2\left(c_{13}+c_{44}\right)\left(R_1+R_3\right)\right],\\
d_0&=c_{44}\left[-c_{11}K_1+\left(R_1+R_3\right)^2\right]-K_2\left[c_{11}c_{33}+c_{44}^2-\left(c_{13}+c_{44}\right)^2\right]\\
&\quad+R_3\left[2c_{11}R_2+c_{44}R_3-2\left(c_{13}+c_{44}\right)\left(R_1+R_3\right)\right],\\
f_0&=c_{11}\left(R_3^2-c_{44}K_2\right).
\end{aligned} \tag{7}$$

The coefficients k_{1j}, k_{2j}, ω_{1j} and ω_{2j} are given by

$$k_{1j} = \frac{c_{11}K_2 + m_3 s_j^2 + c_{44}K_1 s_j^4}{m_2 s_j^3 - m_1 s_j}, \quad k_{2j} = \frac{c_{11}R_3 - m_4 s_j^2 + c_{44}R_2 s_j^4}{m_1 s_j - m_2 s_j^3}$$
$$\omega_{1j} = c_{44}\left(1 + k_{1j}\right) + R_3 k_{2j}, \quad \omega_{2j} = R_3\left(1 + k_{1j}\right) + K_2 k_{2j}, \tag{8}$$

where

$$\begin{aligned} m_1 &= -K_2\left(c_{13} + c_{44}\right) + R_3\left(R_1 + R_3\right), \\ m_2 &= -K_1\left(c_{13} + c_{44}\right) + R_2\left(R_1 + R_3\right), \\ m_3 &= -c_{11}K_1 - c_{44}K_2 + \left(R_1 + R_3\right)^2, \\ m_4 &= c_{11}R_2 + c_{44}R_3 - \left(c_{13} + c_{44}\right)\left(R_1 + R_3\right). \end{aligned} \tag{9}$$

It should be noted that the general solution given in Eq. (3) is only valid for the case of distinct eigenvalues $s_1 \neq s_2 \neq s_3 \neq s_1$ which is the most common case.

2.2. General solution for the transversely isotropic material

When the $r-\phi$ plane is parallel to the isotropic plane of material in cylindrical coordinates (r, ϕ, z), the constitutive relations of transversely isotropic material are:

$$\begin{aligned} \sigma_r' &= c_{11}'\frac{\partial u_r'}{\partial r} + c_{12}'\left(\frac{u_r'}{r} + \frac{1}{r}\frac{\partial u_\phi'}{\partial \phi}\right) + c_{13}'\frac{\partial u_z'}{\partial z}, \quad \tau_{r\phi}' = c_{66}'\left(\frac{1}{r}\frac{\partial u_r'}{\partial \phi} + \frac{\partial u_\phi'}{\partial r} - \frac{u_\phi'}{r}\right), \\ \sigma_\phi' &= c_{12}'\frac{\partial u_r'}{\partial r} + c_{11}'\left(\frac{u_r'}{r} + \frac{1}{r}\frac{\partial u_\phi'}{\partial \phi}\right) + c_{13}'\frac{\partial u_z'}{\partial z}, \quad \tau_{\phi z}' = c_{44}'\left(\frac{\partial u_\phi'}{\partial z} + \frac{1}{r}\frac{\partial u_z'}{\partial \phi}\right), \\ \sigma_z' &= c_{13}'\left(\frac{\partial u_r'}{\partial r} + \frac{u_r'}{r} + \frac{1}{r}\frac{\partial u_\phi'}{\partial \phi}\right) + c_{33}'\frac{\partial u_z'}{\partial z}, \quad \tau_{zr}' = c_{44}'\left(\frac{\partial u_z'}{\partial r} + \frac{\partial u_r'}{\partial z}\right), \end{aligned} \tag{10}$$

where $u_m'(m = r, \phi, z)$ are the components of the displacement; σ_m' and $\tau_{mn}'\,(m, n = r, \phi, z)$ are the components of normal and shear stresses, respectively; $c_{ij}'\,(i, j = 1, 2, \ldots, 6)$ are the elastic moduli. The relation $c_{66}' = (c_{11}' - c_{12}')/2$ holds for transversely isotropic material.

Ignoring the effects of body force, the equilibrium equations are:

$$\begin{aligned} &\frac{\partial \sigma_r'}{\partial r} + \frac{1}{r}\frac{\partial \tau_{r\phi}'}{\partial \phi} + \frac{\partial \tau_{zr}'}{\partial z} + \frac{\sigma_r' - \sigma_\phi'}{r} = 0, \\ &\frac{\partial \tau_{r\phi}'}{\partial r} + \frac{1}{r}\frac{\partial \sigma_\phi'}{\partial \phi} + \frac{\partial \tau_{\phi z}'}{\partial z} + \frac{2\tau_{r\phi}'}{r} = 0, \\ &\frac{\partial \tau_{zr}'}{\partial r} + \frac{1}{r}\frac{\partial \tau_{\phi z}'}{\partial \phi} + \frac{\partial \sigma_z'}{\partial z} + \frac{\tau_{zr}'}{r} = 0. \end{aligned} \tag{11}$$

Ding et al. [54] presented a compact general solution for governing Eqs. (1, 2). As for axisymmetric problem, the corresponding general solution is presented in the following form:

$$u_r' = \sum_{i=1}^{2}\frac{\partial \psi_i'}{\partial r}, \quad u_z' = \sum_{i=1}^{2} s_i' k_i' \frac{\partial \psi_i'}{\partial z_i'}, \quad u_\phi' = 0, \tag{12a}$$

$$\sigma_r' = -2c_{66}'\sum_{j=1}^{2}\frac{1}{r}\frac{\partial \psi_i'}{\partial r} - \sum_{i=1}^{2} s_i'^2 \omega_i' \frac{\partial^2 \psi_i'}{\partial z_i'^2},$$

$$\sigma'_\phi = 2c'_{66}\sum_{i=1}^{2}\frac{1}{r}\frac{\partial\psi'_i}{\partial r} - \sum_{i=1}^{2}(s_i'^2\omega'_i - 2c'_{66})\frac{\partial^2\psi'_i}{\partial z_i'^2},$$

$$\sigma'_z = \sum_{i=1}^{2}\omega'_i\frac{\partial^2\psi'_i}{\partial z_i'^2}, \quad \tau'_{zr} = \sum_{i=1}^{2}s'_i\omega'_i\frac{\partial^2\psi'_i}{\partial r\partial z'_i}, \quad \tau'_{r\phi} = \tau'_{\phi z} = 0, \tag{12b}$$

where $\psi'_i\,(i=1,2)$ are two functions which satisfy following quasiharmonic equations:

$$\left(\frac{\partial^2}{\partial r^2} + \frac{\partial}{r\partial r} + \frac{\partial^2}{\partial z_i'^2}\right)\psi'_i = 0 \quad (i=1,2), \tag{13}$$

and

$$z'_i = s'_i z, \quad (i=1,2). \tag{14}$$

Parameters $s'_i\,(i=1,2)$, which satisfy $\mathrm{Re}(s'_i) > 0$, are two eigenvalues of following algebraic equation of the fourth orders:

$$as'^4 - bs'^2 + c = 0, \tag{15}$$

where

$$a = c'_{33}c'_{44}, \quad b = c'_{11}c'_{33} + c_{44}'^2 - (c'_{13} + c'_{44})^2, \quad c = c'_{11}c'_{44}. \tag{16}$$

In addition,

$$k'_i = \frac{c'_{11} - c'_{44}s_i^2}{(c'_{13} + c'_{44})s_i'^2}, \quad \omega'_i = c'_{33}s_i'^2k'_i - c'_{13}. \tag{17}$$

It should be noted that the general solution given in Eq. (3) is only valid for the case when the eigenvalues $s'_i\,(i=1,2)$ are distinct which is the most common.

There are two different fields coupling in quasicrystals; in order to balance the equations, the constitutive relation of phason field in the transversely isotropic material is introduced.

$$H'_r = K_r\frac{\partial w'}{\partial r}, \quad H'_\phi = K_\phi\frac{1}{r}\frac{\partial w'}{\partial\phi}, \quad H'_z = K_z\frac{\partial w'}{\partial z}, \tag{18}$$

where K_r, K_ϕ, K_z are cooperation constants.

As for axisymmetric problem, $H'_\phi = 0$. The phason equilibrium equation is

$$\frac{1}{r}\frac{\partial}{\partial r}(rH'_r) + \frac{\partial H'_z}{\partial z} = 0. \tag{19}$$

Substituting Eq. (18) into Eq. (19) yields

$$K_r\left(\frac{\partial^2 w'}{\partial^2 r} + \frac{\partial w'}{r\partial r}\right) + K_z\frac{\partial^2 w'}{\partial^2 z} = 0. \tag{20}$$

For the convenience to construct the solution, the function ψ'_δ is introduced

$$w' = s'_\delta\frac{\partial\psi'_\delta}{\partial z'_\delta}, \tag{21}$$

where $s'_\delta = \sqrt{K_r/K_z}$, $z'_\delta = s'_\delta z$, ψ'_δ in Eq. (21) still satisfy following harmonic equation:

$$\left(\frac{\partial^2}{\partial r^2} + \frac{\partial}{r\partial r} + \frac{\partial^2}{\partial z_\delta'^2}\right)\psi'_\delta = 0. \tag{22}$$

Substituting Eq. (21) into Eq. (18) yields

$$H'_z = K_r\frac{\partial^2\psi'_\delta}{\partial z_\delta'^2}, \quad H'_r = s'_\delta K_r\frac{\partial^2\psi'_\delta}{\partial z'_\delta\partial r}. \tag{23}$$

3. Green's function for a normal point force acting on the surface of 1D hexagonal quasicrystal coating

Consider a coating material with thickness h which is perfectly bonded to a semi-infinite substrate $z \leq 0$ (Fig. 1). They are 1D hexagonal quasicrystals with isotropic plane perpendicular to the z axis. The coating material can be modeled as an infinite plate with a free surface $z = h$ and an interface $z = 0$ bonded to semi-infinite substrate $z \leq 0$. A normal point force P_z is applied at the point on the free surface of coating material. This is an axisymmetric problem; the phonon–phason coupling and elastic field in the coating and semi-infinite substrate will be derived based on the axisymmetric general solution $(0, \phi, h)$ on in Eqs. (3,12,23).

The boundary conditions on the free surface $z = h$ are in the form of

$$\sigma_z(r,h) = 0, \quad \tau_{zr}(r,h) = 0,\ H_z(r,h) = 0, \tag{24}$$

when the equilibrium for an infinite layer $\varepsilon \leq z \leq h\,(0 < \varepsilon < h)$ is considered (Fig. 1), the equation should be satisfied as follows:

$$-2\pi \int_0^{+\infty} \sigma_z(r,\varepsilon) r \mathrm{d}r + P_z = 0. \tag{25}$$

The coating material $0 \leq z \leq h$ and the semi-infinite substrate $z \leq 0$ are assumed to be perfectly bonded. The compatibility conditions at the interface $z = 0$ are in form of

$$\begin{aligned} u_r(r,0) &= u_r'(r,0), \quad u_z(r,0) = u_z'(r,0), \\ \sigma_z(r,0) &= \sigma_z'(r,0), \quad \tau_{zr}(r,0) = \tau_{zr}'(r,0), \\ H_z(r,0) &= H_z'(r,0), \quad w(r,0) = w'(r,0), \end{aligned} \tag{26}$$

where the primed quantities refer to the variables in the semi-infinite substrate $z \leq 0$ and the un-primed quantities refer to those in coating material $0 \leq z \leq h$.

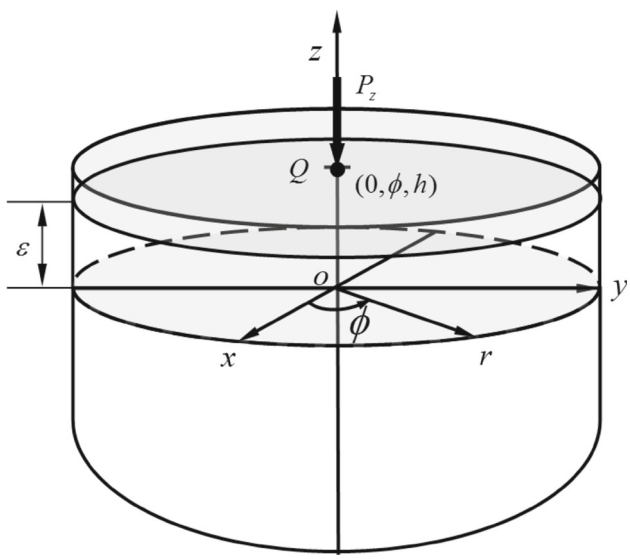

FIG. 1. A normal point force P_z acting on the free surface of a 1D hexagonal quasicrystals coating material

To simplify notations, the following quantities are introduced:

$$
\begin{aligned}
&z_j = s_j z, \quad z'_i = s'_i z, \quad h_j = s_j h, \quad z'_\delta = s'_\delta z\\
&h_{nkl} = (2n-k)h_1 + (k-l)h_2 + (l-1)h_3,\\
&\bar{z}_{njkl} = z_j - h_{nkl}, \quad \bar{R}_{njkl} = \sqrt{r^2 + \bar{z}^2_{njkl}}, \quad \bar{R}^*_{njkl} = \bar{R}_{njkl} - \bar{z}_{njkl},\\
&z_{njkl} = z_j - h_{nkl}, \quad R_{njkl} = \sqrt{r^2 + z^2_{njkl}}, R^*_{njk} = R_{njkl} + z_{njkl},\\
&z'_{nikl} = z'_i - h_{nkl}, \quad R'_{nikl} = \sqrt{r^2 + z'^2_{nikl}}, \quad R'^*_{nikl} = R'_{nikl} - z'_{nikl},\\
&z'_{n\delta kl} = z'_\delta - h_{nkl}, \quad R'_{n\delta kl} = \sqrt{r^2 + z'^2_{n\delta kl}}, \quad R'^*_{n\delta kl} = R'_{n\delta kl} - z'_{n\delta kl},\\
&\qquad (n = 1, 2, \ldots, \infty; j = 1, 2, 3; i = 1, 2; k = 1, 2, \ldots, 2n; l = 1, 2, \ldots, k),
\end{aligned} \tag{27}
$$

where s'_i are the eigenvalues of material in semi-infinite substrate $z \le 0$.

The harmonic functions in the coating material $0 \le z \le h$ can be assumed as

$$
\psi_j = \sum_{n=1}^{\infty} (\bar{\psi}_{nj} + \psi_{nj}), \quad (j = 1, 2, 3), \tag{28}
$$

where

$$
\begin{aligned}
&\bar{\psi}_{nj} = \sum_{k=1}^{2n}\sum_{l=1}^{k} \bar{\mathcal{A}}_{njkl} \ln \bar{R}^*_{njkl}, \quad \psi_{nj} = \sum_{k=1}^{2n}\sum_{l=1}^{k} \mathcal{A}_{njkl} \ln R^*_{njkl},\\
&\qquad (n = 1, 2, \ldots, \infty;\ j = 1, 2, 3;\ k = 1, 2, \ldots, 2n;\ l = 1, 2, \ldots, k),
\end{aligned} \tag{29}
$$

$\bar{\mathcal{A}}_{njkl}$ and $\mathcal{A}_{njkl}$ are constants to be determined, $\bar{R}^*_{njkl}$ and R^*_{njkl} are defined in Eq. (27).

The corresponding phonon–phason coupling and elastic fields can be obtained by the substitution of Eqs. (28, 29) into the general solution in Eq. (3) as follows:

$$
\begin{aligned}
&u_r = \sum_{n=1}^{\infty} (\bar{u}_{rn} + u_{rn}), \quad u_z = \sum_{n=1}^{\infty} (\bar{u}_{zn} + u_{zn}), \qquad \text{(30a)}\\
&w = \sum_{n=1}^{\infty} (\bar{w}_n + w_n), \sigma_r = \sum_{n=1}^{\infty} (\bar{\sigma}_{rn} + \sigma_{rn}), \quad \sigma_\phi = \sum_{n=1}^{\infty} (\bar{\sigma}_{\phi n} + \sigma_{\phi n}),\\
&\sigma_z = \sum_{n=1}^{\infty} (\bar{\sigma}_{zn} + \sigma_{zn}), \quad \tau_{zr} = \sum_{n=1}^{\infty} (\bar{\tau}_{zrn} + \tau_{zrn}),\\
&H_r = \sum_{n=1}^{\infty} \left(\bar{H}_{rn} + H_{rn}\right), \quad H_z = \sum_{n=1}^{\infty} \left(\bar{H}_{zn} + H_{zn}\right), \qquad \text{(30b)}
\end{aligned}
$$

where

$$
\begin{aligned}
&\bar{u}_{rn} = \sum_{j=1}^{3}\sum_{k=1}^{2n}\sum_{l=1}^{k} \bar{\mathcal{A}}_{njkl} \frac{r}{\bar{R}_{njkl}\bar{R}^*_{njkl}}, \quad u_{rn} = \sum_{j=1}^{3}\sum_{k=1}^{2n}\sum_{l=1}^{k} \mathcal{A}_{njkl} \frac{r}{R_{njkl}R^*_{njkl}},\\
&\bar{u}_{zn} = \sum_{j=1}^{3}\sum_{k=1}^{2n}\sum_{l=1}^{k} s_j k_{1j} \bar{\mathcal{A}}_{njkl} \frac{-1}{\bar{R}_{njkl}}, \quad u_{zn} = \sum_{j=1}^{3}\sum_{k=1}^{2n}\sum_{l=1}^{k} s_j k_{1j} \mathcal{A}_{njkl} \frac{1}{R_{njkl}},\\
&\bar{w}_n = \sum_{j=1}^{3}\sum_{k=1}^{2n}\sum_{l=1}^{k} s_j k_{2j} \bar{\mathcal{A}}_{njkl} \frac{-1}{\bar{R}_{njkl}}, \quad \bar{w}_n = \sum_{j=1}^{3}\sum_{k=1}^{2n}\sum_{l=1}^{k} s_j k_{2j} \mathcal{A}_{njkl} \frac{1}{R_{njkl}},
\end{aligned}
$$

$$\bar{\sigma}_{rn} = 2c_{66}\sum_{j=1}^{3}\sum_{k=1}^{2n}\sum_{l=1}^{k}\bar{\mathcal{A}}_{njkl}\frac{-1}{\bar{R}_{njkl}\bar{R}^{*}_{njkl}} + \sum_{j=1}^{3}\sum_{k=1}^{2n}\sum_{l=1}^{k}s_j^2\omega_{1j}\bar{\mathcal{A}}_{njkl}\frac{-\bar{z}_{njkl}}{\bar{R}^{3}_{njkl}},$$

$$\sigma_{rn} = 2c_{66}\sum_{j=1}^{3}\sum_{k=1}^{2n}\sum_{l=1}^{k}\mathcal{A}_{njkl}\frac{-1}{R_{njkl}R^{*}_{njkl}} + \sum_{j=1}^{3}\sum_{k=1}^{2n}\sum_{l=1}^{k}s_j^2\omega_{1j}\mathcal{A}_{njkl}\frac{z_{njkl}}{R^{3}_{njkl}},$$

$$\bar{\sigma}_{\phi n} = 2c_{66}\sum_{j=1}^{3}\sum_{k=1}^{2n}\sum_{l=1}^{k}\bar{\mathcal{A}}_{njkl}\frac{1}{\bar{R}_{njkl}\bar{R}^{*}_{njkl}} + \sum_{j=1}^{3}\sum_{k=1}^{2n}\sum_{l=1}^{k}(s_j^2\omega_{1j}-2c_{66})\bar{\mathcal{A}}_{njkl}\frac{-\bar{z}_{njkl}}{\bar{R}^{3}_{njkl}},$$

$$\sigma_{\phi n} = 2c_{66}\sum_{j=1}^{3}\sum_{k=1}^{2n}\sum_{l=1}^{k}\mathcal{A}_{njkl}\frac{1}{R_{njkl}R^{*}_{njkl}} + \sum_{j=1}^{3}\sum_{k=1}^{2n}\sum_{l=1}^{k}(s_j^2\omega_{1j}-2c_{66})\mathcal{A}_{njkl}\frac{z_{njkl}}{R^{3}_{njkl}},$$

$$\bar{\sigma}_{zn} = \sum_{j=1}^{3}\sum_{k=1}^{2n}\sum_{l=1}^{k}\omega_{1j}\bar{\mathcal{A}}_{njkl}\frac{\bar{z}_{njkl}}{\bar{R}^{3}_{njkl}}, \quad \sigma_{zn} = \sum_{j=1}^{3}\sum_{k=1}^{2n}\sum_{l=1}^{k}\omega_{1j}\mathcal{A}_{njkl}\frac{-z_{njkl}}{R^{3}_{njkl}},$$

$$\bar{\tau}_{zrn} = \sum_{j=1}^{3}\sum_{k=1}^{2n}\sum_{l=1}^{k}s_j\omega_{1j}\bar{\mathcal{A}}_{njkl}\frac{r}{\bar{R}^{3}_{njkl}}, \quad \tau_{zrn} = \sum_{j=1}^{3}\sum_{k=1}^{2n}\sum_{l=1}^{k}s_j\omega_{1j}\mathcal{A}_{njkl}\frac{-r}{R^{3}_{njkl}},$$

$$\bar{H}_{rn} = \sum_{j=1}^{3}\sum_{k=1}^{2n}\sum_{l=1}^{k}s_j\omega_{2j}\bar{\mathcal{A}}_{njkl}\frac{r}{\bar{R}^{3}_{njkl}}, \quad \bar{H}_{rn} = \sum_{j=1}^{3}\sum_{k=1}^{2n}\sum_{l=1}^{k}s_j\omega_{2j}\mathcal{A}_{njkl}\frac{-r}{R^{3}_{njkl}},$$

$$\bar{H}_{zn} = \sum_{j=1}^{3}\sum_{k=1}^{2n}\sum_{l=1}^{k}\omega_{2j}\bar{\mathcal{A}}_{njkl}\frac{\bar{z}_{njkl}}{\bar{R}^{3}_{njkl}}, \quad H_{zn} = \sum_{j=1}^{3}\sum_{k=1}^{2n}\sum_{l=1}^{k}\omega_{2j}\mathcal{A}_{njkl}\frac{-z_{njkl}}{R^{3}_{njkl}},$$

$$(n = 1, 2, \cdots, \infty). \tag{31}$$

The harmonic functions in the semi-infinite substrate $z \le 0$ can be assumed as

$$\psi'_i = \sum_{n=1}^{\infty}\psi'_{ni}, (i = 1, 2), \tag{32a}$$

$$\psi'_\delta = \sum_{n=1}^{\infty}\psi'_{n\delta}, \tag{32b}$$

where

$$\psi'_{ni} = \sum_{k=1}^{2n}\sum_{l=1}^{k}\mathcal{A}'_{nikl}\ln R'^{*}_{nikl},$$

$$\psi'_{n\delta} = \sum_{k=1}^{2n}\sum_{l=1}^{k}\mathcal{A}'_{n\delta kl}\ln R'^{*}_{n\delta kl},$$

$$(n = 1, 2, \ldots, \infty;\ i = 1, 2), \tag{33}$$

$\mathcal{A}'_{njk}$ are constants to be determined, R'^{*}_{njk} are defined in Eq. (27).

Substituting Eqs. (32, 33) into general solution (12,23) yields

$$u'_r = \sum_{n=1}^{\infty}u'_{rn}, \quad u'_z = \sum_{n=1}^{\infty}u'_{zn},$$

$$w' = \sum_{n=1}^{\infty}w'_n, \tag{34a}$$

$$\sigma'_r = \sum_{n=1}^{\infty} \sigma'_{rn}, \quad \sigma'_\phi = \sum_{n=1}^{\infty} \sigma'_{\phi n},$$
$$\sigma'_z = \sum_{n=1}^{\infty} \sigma'_{zn}, \quad \tau'_{zr} = \sum_{n=1}^{\infty} \tau'_{zrn},$$
$$H'_r = \sum_{n=1}^{\infty} H'_{rn}, \quad H'_z = \sum_{n=1}^{\infty} H'_{zn}, \tag{34b}$$

where

$$u'_{rn} = \sum_{i=1}^{2}\sum_{k=1}^{2n}\sum_{l=1}^{k} \mathcal{A}'_{nikl} \frac{r}{R'_{nikl} R'^{*}_{nikl}}, \quad u'_{zn} = \sum_{i=1}^{2}\sum_{k=1}^{2n}\sum_{l=1}^{k} s'_i k'_i \mathcal{A}'_{nikl} \frac{-1}{R'_{nikl}},$$
$$\sigma'_{rn} = 2c'_{66} \sum_{i=1}^{2}\sum_{k=1}^{2n}\sum_{l=1}^{k} \mathcal{A}'_{nikl} \frac{-1}{R'_{nikl} R'^{*}_{nikl}} + \sum_{i=1}^{2}\sum_{k=1^{2n}}\sum_{l=1}^{k} s'^{2}_i \omega'_i \mathcal{A}'_{nikl} \frac{-z'_{nikl}}{R'^{3}_{nikl}},$$
$$\sigma'_{\phi n} = 2c'_{66} \sum_{i=1}^{2}\sum_{k=1}^{2n}\sum_{l=1}^{k} \mathcal{A}'_{nikl} \frac{1}{R'_{nikl} R'^{*}_{nikl}} + \sum_{i=1}^{2}\sum_{k=1}^{2n}\sum_{l=1}^{k} (s'^{2}_i \omega'_i - 2c'_{66}) \mathcal{A}'_{nikl} \frac{-z'_{nikl}}{R'^{3}_{nikl}},$$
$$\sigma'_{zn} = \sum_{i=1}^{2}\sum_{k=1}^{2n}\sum_{l=1}^{k} \omega'_i \mathcal{A}'_{nikl} \frac{z'_{nikl}}{R'^{3}_{nikl}}, \quad \tau'_{zrn} = \sum_{i=1}^{2}\sum_{k=1}^{2n}\sum_{l=1}^{k} s'_i \omega'_i \mathcal{A}'_{nikl} \frac{r}{R'^{3}_{nikl}},$$
$$w'_n = \sum_{k=1}^{2n}\sum_{l=1}^{k} s'_\delta \mathcal{A}'_{n\delta kl} \frac{-1}{R'_{n\delta kl}},$$
$$H'_{rn} = \sum_{k=1}^{2n}\sum_{l=1}^{k} s'_\delta K_r \mathcal{A}'_{n\delta kl} \frac{r}{R'_{n\delta kl^3}}, \quad H'_{zn} = \sum_{k=1}^{2n}\sum_{l=1}^{k} K_r \mathcal{A}'_{n\delta kl} \frac{z'_{n\delta kl}}{R'_{n\delta kl^3}},$$
$$(n = 1, 2, \ldots, \infty). \tag{35}$$

Considering the form of Eq. (30), the boundary conditions in Eq. (24) for free surface $z = h$ can be separated into following form:

$$\bar{\sigma}_{z1}(r,h) = 0, \quad \bar{\tau}_{zr1}(r,h) = 0, \quad \bar{H}_{z1}(r,h) = 0, \tag{36a}$$
$$\sigma_{zn}(r,h) + \bar{\sigma}_{z(n+1)}(r,h) = 0, \quad \tau_{zrn}(r,h) + \bar{\tau}_{zr(n+1)}(r,h) = 0,$$
$$H_{zn}(r,h) + \bar{H}_{z(n+1)}(r,h) = 0, \ (n = 1, 2, \ldots, \infty). \tag{36b}$$

Considering the form of Eqs. (30, 34), the compatibility conditions in Eq. (36) for interface $z = 0$ can be separated into following form:

$$\bar{u}_{rn}(r,0) + u_{rn}(r,0) = u'_{rn}(r,0), \quad \bar{u}_{zn}(r,0) + u_{zn}(r,0) = u'_{zn}(r,0),$$
$$\bar{\sigma}_{zn}(r,0) + \sigma_{zn}(r,0) = \sigma'_{zn}(r,0), \quad \bar{\tau}_{zrn}(r,0) + \tau_{zrn}(r,0) = \tau'_{zrn}(r,0),$$
$$\bar{H}_{zn}(r,0) + H_{zn}(r,0) = H'_{zn}(r,0), \quad \bar{w}_n(r,0) + w_n(r,0) = w'_n(r,0),$$
$$(n = 1, 2, \ldots, \infty). \tag{37}$$

Substitution of Eq. (31) into Eq. (36a) gives

$$\bar{\mathcal{A}}_{1121} = \bar{\mathcal{A}}_{1122} = \bar{\mathcal{A}}_{1211} = \bar{\mathcal{A}}_{1222} = \bar{\mathcal{A}}_{1311} = \bar{\mathcal{A}}_{1321} = 0, \tag{38}$$
$$s_1\omega_{11}\bar{\mathcal{A}}_{1111} + s_2\omega_{12}\bar{\mathcal{A}}_{1221} + s_3\omega_{13}\bar{\mathcal{A}}_{1322} = 0. \tag{39}$$

Substituting Eq. (31) into Eq. (36b) with using following identities:

$$
\begin{aligned}
&\bar{z}_{(n+1)1(2n+2)\lambda}(h) = h_1 - (2n+2-\lambda)h_2 - (\lambda-1)h_3,\\
&\bar{z}_{(n+1)2\lambda\lambda}(h) = -(2n+2-\lambda)h_1 + h_2 - (\lambda-1)h_3,\\
&\bar{z}_{(n+1)3\lambda1}(h) = -(2n+2-\lambda)h_1 - (\lambda-1)h_2 + h_3,\\
&\qquad (n=1,2,\ldots,\infty;\ \lambda=1,2,\ldots,2n+2),
\end{aligned}
\tag{40a}
$$

$$
\begin{aligned}
&z_{n111}(h) = -\bar{z}_{(n+1)111}(h) = -\bar{z}_{(n+1)221}(h) = -\bar{z}_{(n+1)322}(h) = 2nh_1,\\
&z_{n2(2n)1}(h) = -\bar{z}_{(n+1)1(2n+1)1}(h) = -\bar{z}_{(n+1)2(2n+2)1}(h) = -\bar{z}_{(n+1)3(2n+2)2}(h) = 2nh_2,\\
&z_{n3(2n)(2n)}(h) = -\bar{z}_{(n+1)1(2n+1)(2n+1)}(h) = -\bar{z}_{(n+1)2(2n+2)(2n+1)}(h) = -\bar{z}_{(n+1)3(2n+2)(2n+2)}(h) = 2nh_3,\\
&z_{n1(m+1)1}(h) = z_{n2m1}(h) = -\bar{z}_{(n+1)1(m+1)1}(h) = -\bar{z}_{(n+1)2(m+2)1}(h) = -\bar{z}_{(n+1)3(m+2)2}(h)\\
&\quad = (2n-m)h_1 + mh_2,\\
&z_{n1(m+1)(m+1)}(h) = z_{n3mm}(h) = -\bar{z}_{(n+1)1(m+1)(m+1)}(h)\\
&\quad = -\bar{z}_{(n+1)2(m+2)(m+1)}(h) = -\bar{z}_{(n+1)3(m+2)(m+2)}(h) = (2n-m)h_1 + mh_3,\\
&z_{n2(2n)(m+1)}(h) = z_{n3(2n)m}(h) = -\bar{z}_{(n+1)1(2n+1)(m+1)}(h) = -\bar{z}_{(n+1)2(2n+2)(m+1)}(h)\\
&\quad = -\bar{z}_{(n+1)3(2n+2)(m+2)}(h) = (2n-m)h_2 + mh_3,\\
&z_{n1(\alpha+1)(\beta+1)}(h) = z_{n2\alpha(\beta+1)}(h) = z_{n3\alpha\beta}(h)\\
&\quad = -\bar{z}_{(n+1)1(\alpha+1)(\beta+1)}(h) = -\bar{z}_{(n+1)2(\alpha+2)(\beta+1)}(h) = (2n-\alpha)h_1 + (\alpha-\beta)h_2 + \beta h_3,\\
&\qquad (n=1,2,\ldots,\infty;\ m=1,2,\ldots,2n-1;\ \alpha=2,3,\ldots,2n-1;\ \beta=1,2,\ldots,\alpha-1),
\end{aligned}
\tag{40b}
$$

one can obtain

$$
\begin{aligned}
&\bar{\mathcal{A}}_{(n+1)1(2n+2)\lambda} = \bar{\mathcal{A}}_{(n+1)2\lambda\lambda} = \bar{\mathcal{A}}_{(n+1)3\lambda1} = 0,\ (n=1,2,\ldots,\infty;\ \lambda=1,2,\ldots,2n+2),\\
&\omega_{11}\bar{\mathcal{A}}_{(n+1)111} + \omega_{12}\bar{\mathcal{A}}_{(n+1)221} + \omega_{13}\bar{\mathcal{A}}_{(n+1)322} = -\omega_{11}\mathcal{A}_{n111},
\end{aligned}
\tag{41a}
$$

$$
\begin{aligned}
&\omega_{11}\bar{\mathcal{A}}_{(n+1)1(2n+1)1} + \omega_{12}\bar{\mathcal{A}}_{(n+1)2(2n+2)1} + \omega_{13}\bar{\mathcal{A}}_{(n+1)3(2n+2)2} = -\omega_{12}\mathcal{A}_{n2(2n)1},\\
&\omega_{11}\bar{\mathcal{A}}_{(n+1)1(2n+1)(2n+1)} + \omega_{12}\bar{\mathcal{A}}_{(n+1)2(2n+2)(2n+1)} + \omega_{13}\bar{\mathcal{A}}_{(n+1)3(2n+2)(2n+2)} = -\omega_{13}\mathcal{A}_{n3(2n)(2n)},\\
&\omega_{11}\bar{\mathcal{A}}_{(n+1)1(m+1)1} + \omega_{12}\bar{\mathcal{A}}_{(n+1)2(m+2)1} + \omega_{13}\bar{\mathcal{A}}_{(n+1)3(m+2)2} = -\left(\omega_{11}\mathcal{A}_{n1(m+1)1} + \omega_{12}\mathcal{A}_{n2m1}\right),\\
&\omega_{11}\bar{\mathcal{A}}_{(n+1)1(m+1)(m+1)} + \omega_{12}\bar{\mathcal{A}}_{(n+1)2(m+2)(m+1)} + \omega_{13}\bar{\mathcal{A}}_{(n+1)3(m+2)(m+2)}\\
&= -\left(\omega_{11}\mathcal{A}_{n1(m+1)(m+1)} + \omega_{13}\mathcal{A}_{n3mm}\right),\\
&\omega_{11}\bar{\mathcal{A}}_{(n+1)1(2n+1)(m+1)} + \omega_{12}\bar{\mathcal{A}}_{(n+1)2(2n+2)(m+1)} + \omega_{13}\bar{\mathcal{A}}_{(n+1)3(2n+2)(m+2)}\\
&\quad = -\left(\omega_{12}\mathcal{A}_{n2(2n)(m+1)} + \omega_{13}\mathcal{A}_{n3(2n)m}\right),\\
&\omega_{11}\bar{\mathcal{A}}_{(n+1)1(\alpha+1)(\beta+1)} + \omega_{12}\bar{\mathcal{A}}_{(n+1)2(\alpha+2)(\beta+1)} + \omega_{13}\bar{\mathcal{A}}_{(n+1)3(\alpha+2)(\beta+2)}\\
&\quad = -\left(\omega_{11}\mathcal{A}_{n1(\alpha+1)(\beta+1)} + \omega_{12}\mathcal{A}_{n2\alpha(\beta+1)} + \omega_{13}\mathcal{A}_{n3\alpha\beta}\right),\\
&(n=1,2,\ldots,\infty;\ m=1,2,\ldots,2n-1;\ \alpha=2,3,\ldots,2n-1;\ \beta=1,2,\ldots,\alpha-1),
\end{aligned}
\tag{41b}
$$

$$
\begin{aligned}
&s_1\omega_{11}\bar{\mathcal{A}}_{(n+1)111} + s_2\omega_{12}\bar{\mathcal{A}}_{(n+1)221} + s_3\omega_{13}\bar{\mathcal{A}}_{(n+1)322} = s_1\omega_{11}\mathcal{A}_{n111},\\
&s_1\omega_{11}\bar{\mathcal{A}}_{(n+1)1(2n+1)1} + s_2\omega_{12}\bar{\mathcal{A}}_{(n+1)2(2n+2)1} + s_3\omega_{13}\bar{\mathcal{A}}_{(n+1)3(2n+2)2} = s_2\omega_{12}\mathcal{A}_{n2(2n)1},\\
&s_1\omega_{11}\bar{\mathcal{A}}_{(n+1)1(2n+1)(2n+1)} + s_2\omega_{12}\bar{\mathcal{A}}_{(n+1)2(2n+2)(2n+1)} + s_3\omega_{13}\bar{\mathcal{A}}_{(n+1)3(2n+2)(2n+2)} = s_3\omega_{13}\mathcal{A}_{n3(2n)(2n)},\\
&s_1\omega_{11}\bar{\mathcal{A}}_{(n+1)1(m+1)1} + s_2\omega_{12}\bar{\mathcal{A}}_{(n+1)2(m+2)1} + s_3\omega_{13}\bar{\mathcal{A}}_{(n+1)3(m+2)2}\\
&\quad = s_1\omega_{11}\mathcal{A}_{n1(m+1)1} + s_2\omega_{12}\mathcal{A}_{n2m1},\\
&s_1\omega_{11}\bar{\mathcal{A}}_{(n+1)1(m+1)(m+1)} + s_2\omega_{12}\bar{\mathcal{A}}_{(n+1)2(m+2)(m+1)} + s_3\omega_{13}\bar{\mathcal{A}}_{(n+1)3(m+2)(m+2)}\\
&\quad = s_1\omega_{11}\mathcal{A}_{n1(m+1)(m+1)} + s_3\omega_{13}\mathcal{A}_{n3mm},\\
&s_1\omega_{11}\bar{\mathcal{A}}_{(n+1)1(2n+1)(m+1)} + s_2\omega_{12}\bar{\mathcal{A}}_{(n+1)2(2n+2)(m+1)} + s_3\omega_{13}\bar{\mathcal{A}}_{(n+1)3(2n+2)(m+2)}
\end{aligned}
$$

$$
\begin{aligned}
&= s_2\omega_{12}\mathcal{A}_{n2(2n)(m+1)}+s_3\omega_{13}\mathcal{A}_{n3(2n)m},\\
&s_1\omega_{11}\bar{\mathcal{A}}_{(n+1)1(\alpha+1)(\beta+1)} + s_2\omega_{12}\bar{\mathcal{A}}_{(n+1)2(\alpha+2)(\beta+1)} + s_3\omega_{13}\bar{\mathcal{A}}_{(n+1)3(\alpha+2)(\beta+2)}\\
&= s_1\omega_{11}\mathcal{A}_{n1(\alpha+1)(\beta+1)}+s_2\omega_{12}\mathcal{A}_{n2\alpha(\beta+1)}+s_3\omega_{13}\mathcal{A}_{n3\alpha\beta},\\
&(n=1,2,\ldots,\infty;\ m=1,2,\ldots,2n-1;\ \alpha=2,3,\ldots,2n-1;\ \beta=1,2,\ldots,\alpha-1),
\end{aligned}
\tag{41c}
$$

$$
\begin{aligned}
&\omega_{21}\bar{\mathcal{A}}_{(n+1)111} + \omega_{22}\bar{\mathcal{A}}_{(n+1)221} + \omega_{23}\bar{\mathcal{A}}_{(n+1)322} = -\omega_{21}\mathcal{A}_{n111},\\
&\omega_{21}\bar{\mathcal{A}}_{(n+1)1(2n+1)1} + \omega_{22}\bar{\mathcal{A}}_{(n+1)2(2n+2)1} + \omega_{23}\bar{\mathcal{A}}_{(n+1)3(2n+2)2} = -\omega_{22}\mathcal{A}_{n2(2n)1},\\
&\omega_{21}\bar{\mathcal{A}}_{(n+1)1(2n+1)(2n+1)} + \omega_{22}\bar{\mathcal{A}}_{(n+1)2(2n+2)(2n+1)} + \omega_{23}\bar{\mathcal{A}}_{(n+1)3(2n+2)(2n+2)} = -\omega_{23}\mathcal{A}_{n3(2n)(2n)},\\
&\omega_{21}\bar{\mathcal{A}}_{(n+1)1(m+1)1} + \omega_{22}\bar{\mathcal{A}}_{(n+1)2(m+2)1} + \omega_{23}\bar{\mathcal{A}}_{(n+1)3(m+2)2} = -\left(\omega_{21}\mathcal{A}_{n1(m+1)1} + \omega_{22}\mathcal{A}_{n2m1}\right),\\
&\omega_{21}\bar{\mathcal{A}}_{(n+1)1(m+1)(m+1)} + \omega_{22}\bar{\mathcal{A}}_{(n+1)2(m+2)(m+1)} + \omega_{23}\bar{\mathcal{A}}_{(n+1)3(m+2)(m+2)}\\
&\quad = -\left(\omega_{21}\mathcal{A}_{n1(m+1)(m+1)} + \omega_{23}\mathcal{A}_{n3mm}\right)\\
&\omega_{21}\bar{\mathcal{A}}_{(n+1)1(2n+1)(m+1)} + \omega_{22}\bar{\mathcal{A}}_{(n+1)2(2n+2)(m+1)} + \omega_{23}\bar{\mathcal{A}}_{(n+1)3(2n+2)(m+2)}\\
&\quad = -\left(\omega_{22}\mathcal{A}_{n2(2n)(m+1)} + \omega_{23}\mathcal{A}_{n3(2n)m}\right),\\
&\omega_{21}\bar{\mathcal{A}}_{(n+1)1(\alpha+1)(\beta+1)} + \omega_{22}\bar{\mathcal{A}}_{(n+1)2(\alpha+2)(\beta+1)} + \omega_{23}\bar{\mathcal{A}}_{(n+1)3(\alpha+2)(\beta+2)}\\
&\quad = -\left(\omega_{21}\mathcal{A}_{n1(\alpha+1)(\beta+1)} + \omega_{22}\mathcal{A}_{n2\alpha(\beta+1)} + \omega_{23}\mathcal{A}_{n3\alpha\beta}\right),\\
&(n=1,2,\ldots,\infty;\ m=1,2,\ldots,2n-1;\ \alpha=2,3,\ldots,2n-1;\ \beta=1,2,\ldots,\alpha-1).
\end{aligned}
\tag{41d}
$$

Substituting Eqs. (31, 35) into Eq. (37) with using following identities:

$$
\begin{aligned}
\bar{z}_{njkl}(0) &= -z_{njkl}(0) = z'_{nikl}(0) = z'_{n\delta kl}(0) = -h_{nkl},\\
\bar{R}_{njkl}(r,0) &= R_{njkl}(r,0) = R'_{nikl}(r,0) = R'_{n\delta kl}(r,0) = \sqrt{r^2+h_{nkl}^2},\\
\bar{R}^*_{njkl}(r,0) &= R^*_{njkl}(r,0) = R'^*_{nikl}(r,0) = R'^*_{n\delta kl}(r,0) = \sqrt{r^2+h_{nkl}^2} + h_{nkl},\\
&\quad (n=1,2,\ldots,\infty;\ i=1,2;\ k=1,2,\ldots,2n;\ l=1,2,\ldots,k),
\end{aligned}
\tag{42}
$$

one can obtain

$$
\begin{aligned}
&\sum_{j=1}^{3}\left(\bar{\mathcal{A}}_{njkl}+\mathcal{A}_{njkl}\right) = \sum_{i=1}^{2}\mathcal{A}'_{nikl},\\
&\sum_{j=1}^{3}\left(s_jk_{1j}\bar{\mathcal{A}}_{njkl}-s_jk_{1j}\mathcal{A}_{njkl}\right) = \sum_{i=1}^{2}s'_ik'_i\mathcal{A}'_{nikl},\\
&\sum_{j=1}^{3}\left(\omega_{1j}\bar{\mathcal{A}}_{njkl}+\omega_{1j}\mathcal{A}_{njkl}\right) = \sum_{i=1}^{2}\omega'_i\mathcal{A}'_{nikl},\\
&\sum_{j=1}^{3}\left(s_j\omega_{1j}\bar{\mathcal{A}}_{njkl}-s_j\omega_{1j}\mathcal{A}_{njkl}\right) = \sum_{i=1}^{2}s'_i\omega'_i\mathcal{A}'_{nikl},\\
&\sum_{j=1}^{3}\left(\omega_{2j}\bar{\mathcal{A}}_{njkl}+\omega_{2j}\mathcal{A}_{njkl}\right) = K_r\mathcal{A}'_{n\delta kl},\\
&\sum_{j=1}^{3}\left(s_jk_{2j}\bar{\mathcal{A}}_{njkl}-s_jk_{2j}\mathcal{A}_{njkl}\right) = s'_\delta\mathcal{A}'_{n\delta kl},\\
&\quad (n=1,2,\ldots,\infty;\ j=1,2,3;\ k=1,2,\ldots,2n;\ l=1,2,\ldots,k).
\end{aligned}
\tag{43}
$$

Substituting Eq. (31) into equilibrium Eq. (25) with using following integral:

$$\int \frac{\bar{z}_{njkl}}{\bar{R}^3_{njkl}} r dr = -\frac{\bar{z}_{njkl}}{\bar{R}_{njkl}}, \quad \int \frac{z_{njkl}}{R^3_{njkl}} r dr = -\frac{z_{njkl}}{R_{njkl}}, \tag{44}$$

one can obtain

$$\sum_{n=1}^{\infty}\sum_{j=1}^{3}\sum_{k=1}^{2n}\sum_{l=1}^{k}\omega_{1j}\left[\bar{\mathcal{A}}_{njkl}\frac{\bar{z}_{njkl}(\varepsilon)}{\bar{R}_{njkl}(r,\varepsilon)} - \mathcal{A}_{njkl}\frac{z_{njkl}(\varepsilon)}{R_{njkl}(r,\varepsilon)}\right]_{r=0}^{r=+\infty} = -\frac{P_z}{2\pi}. \tag{45}$$

Using following limits:

$$\lim_{r\to\infty}\frac{\bar{z}_{njkl}(\varepsilon)}{\bar{R}_{njkl}(r,\varepsilon)} = \lim_{r\to\infty}\frac{z_{njkl}(\varepsilon)}{R_{njkl}(r,\varepsilon)} = 0, \quad \lim_{r\to 0}\frac{\bar{z}_{njkl}(\varepsilon)}{\bar{R}_{njkl}(r,\varepsilon)} = -1, \quad \lim_{r\to 0}\frac{z_{njkl}(\varepsilon)}{R_{njkl}(r,\varepsilon)} = 1,$$
$$(n = 1, 2, \ldots, \infty;\ j = 1, 2;\ k = 1, 2, \ldots, 2n), \tag{46}$$

Eq. (45) can be transferred into

$$\sum_{n=1}^{\infty}\sum_{j=1}^{3}\sum_{k=1}^{2n}\sum_{l=1}^{k}\omega_{1j}\left(\bar{\mathcal{A}}_{njkl} + \mathcal{A}_{njkl}\right) = -\frac{P_z}{2\pi}. \tag{47}$$

Using Eqs. (38,41) and following identities:

$$\begin{aligned}
&\sum_{n=1}^{\infty}\sum_{j=1}^{3}\sum_{k=1}^{2n}\sum_{l=1}^{k}\omega_{1j}\left(\bar{\mathcal{A}}_{njkl} + \mathcal{A}_{njkl}\right) = \sum_{j=1}^{3}\sum_{k=1}^{2}\sum_{l=1}^{k}\omega_{1j}\bar{\mathcal{A}}_{1jkl}\\
&+\sum_{n=1}^{\infty}\sum_{\lambda=1}^{2n+2}\omega_{11}\bar{\mathcal{A}}_{(n+1)1(2n+2)\lambda} + \sum_{n=1}^{\infty}\sum_{\lambda=1}^{2n+2}\omega_{12}\bar{\mathcal{A}}_{(n+1)2\lambda\lambda} + \sum_{n=1}^{\infty}\sum_{\lambda=1}^{2n+2}\omega_{13}\bar{\mathcal{A}}_{(n+1)3\lambda 1}\\
&+\sum_{n=1}^{\infty}\left(\omega_{11}\bar{\mathcal{A}}_{(n+1)111} + \omega_{12}\bar{\mathcal{A}}_{(n+1)221} + \omega_{13}\bar{\mathcal{A}}_{(n+1)322} + \omega_{1}\mathcal{A}_{n111}\right)\\
&+\sum_{n=1}^{\infty}\left(\omega_{11}\bar{\mathcal{A}}_{(n+1)1(2n+1)1} + \omega_{12}\bar{\mathcal{A}}_{(n+1)2(2n+2)1} + \omega_{13}\bar{\mathcal{A}}_{(n+1)3(2n+2)2} + \omega_{12}\mathcal{A}_{n2(2n)1}\right)\\
&+\sum_{n=1}^{\infty}\left(\omega_{11}\bar{\mathcal{A}}_{(n+1)1(2n+1)(2n+1)} + \omega_{12}\bar{\mathcal{A}}_{(n+1)2(2n+2)(2n+1)} + \omega_{13}\bar{\mathcal{A}}_{(n+1)3(2n+2)(2n+2)} + \omega_{13}\mathcal{A}_{n3(2n)(2n)}\right)\\
&+\sum_{n=1}^{\infty}\sum_{m=1}^{2n-1}\left(\omega_{11}\bar{\mathcal{A}}_{(n+1)1(m+1)1} + \omega_{12}\bar{\mathcal{A}}_{(n+1)2(m+2)1} + \omega_{13}\bar{\mathcal{A}}_{(n+1)3(m+2)2} + \omega_{11}\mathcal{A}_{n1(m+1)1} + \omega_{12}\mathcal{A}_{n2m1}\right)\\
&+\sum_{n=1}^{\infty}\sum_{m=1}^{2n-1}\left(\omega_{11}\bar{\mathcal{A}}_{(n+1)1(m+1)(m+1)} + \omega_{12}\bar{\mathcal{A}}_{(n+1)2(m+2)(m+1)} + \omega_{13}\bar{\mathcal{A}}_{(n+1)3(m+2)(m+2)}\right.\\
&\left.+\omega_{11}\mathcal{A}_{n1(m+1)(m+1)} + \omega_{13}\mathcal{A}_{n3mm}\right)\\
&+\sum_{n=1}^{\infty}\sum_{m=1}^{2n-1}\left(\omega_{11}\bar{\mathcal{A}}_{(n+1)1(2n+1)(m+1)} + \omega_{12}\bar{\mathcal{A}}_{(n+1)2(2n+2)(m+1)} + \omega_{13}\bar{\mathcal{A}}_{(n+1)3(2n+2)(m+2)}\right.\\
&\left.+\omega_{12}\mathcal{A}_{n2(2n)(m+1)} + \omega_{13}\mathcal{A}_{n3(2n)m}\right)\\
&+\sum_{n=1}^{\infty}\sum_{\alpha=2}^{2n-1}\sum_{\beta=1}^{\alpha-1}\left(\omega_{11}\bar{\mathcal{A}}_{(n+1)1(\alpha+1)(\beta+1)} + \omega_{12}\bar{\mathcal{A}}_{(n+1)2(\alpha+2)(\beta+1)} + \omega_{13}\bar{\mathcal{A}}_{(n+1)3(\alpha+2)(\beta+2)}\right.\\
&\left.+\omega_{11}\mathcal{A}_{n1(\alpha+1)(\beta+1)} + \omega_{12}\mathcal{A}_{n2\alpha(\beta+1)} + \omega_{13}\mathcal{A}_{n3\alpha\beta}\right),
\end{aligned} \tag{48}$$

Table 1. *Material property of 1D hexagonal quasicrystals* [58]

1D hexagonal quasicrystals	Numerical value
phonon elastic constants (10^9 N/m^2)	$c_{11} = 150, c_{12} = 100, c_{13} = 90$ $c_{33} = 130, c_{44} = 50$
phason elastic constants (10^9 N/m^2)	$K_1 = 0.3, K_2 = 0.18$
phonon–phason coupling constants (10^9 N/m^2)	$R_1 = -1.50, R_2 = 1.20, R_3 = 1.20$

Table 2. *Material property of steel* [59]

Steel	Numerical value
Elastic modulus (10^9 N/m^2)	206
Shear modulus (10^9 N/m^2)	79.23
Poisson's ratio	0.3
Cooperation constants (10^{-11} N/m^2)	$K_r = 17, K_z = 25$

Equation (47) can be simplified to

$$\omega_{11}\bar{\mathcal{A}}_{1111} + \omega_{12}\bar{\mathcal{A}}_{1221} + \omega_{13}\bar{\mathcal{A}}_{1322} = -\frac{P_z}{2\pi}. \tag{49}$$

Thus, $\bar{\mathcal{A}}_{1jkl}$ $(j = 1, 2, 3;\ i = 1, 2;\ k = 1, 2;\ l = 1, 2)$ can be determined by these 9 equations in Eqs. (38, 39, 49). Then, $\mathcal{A}_{1jkl}$, $\mathcal{A}'_{1ikl}$ and $\mathcal{A}'_{1\delta kl}$ $(j = 1, 2, 3;\ i = 1, 2;\ k = 1, 2;\ l = 1, 2)$ can be determined by these 6 equations in Eq. (43). And then, $\bar{\mathcal{A}}_{2jkl}$ $(j = 1, 2, 3;\ i = 1, 2;\ k = 1, 2;\ l = 1, 2, \ldots k)$ can be determined by these 24 equations in Eq. (41). Therefore, for an arbitrary n, $\mathcal{A}_{njk}$ and $\mathcal{A}'_{njk}$ $(j = 1, 2, 3;\ k = 1, 2, \ldots, 2n;\ l = 1, 2, \ldots k)$ can be determined by those recursive equations in Eq. (43), and $\bar{\mathcal{A}}_{(n+1)jk}$ $(j = 1, 2, 3;\ k = 1, 2, \ldots, 2n;\ l = 1, 2, \ldots, k)$ can be determined by those recursive equations in Eq. (41). Thus, the phonon–phason coupling and elastic field of Eqs. (30, 31) in the coating material $0 \le z \le h$ and the phonon–phason coupling and elastic field of Eqs. (34, 35) in semi-infinite substrate $z \le 0$ can be determined.

4. Numerical results

By virtue of the solutions derived above, some further numerical analysis is made. According to the relationship between computational accuracy and iterations, a more precise conclusion about the influence of the coating thickness as well as the magnitude of the force on the distribution of stresses and displacement on the interface can be obtained. Thus, the coating thickness, according to the different load, can be determined in practical applications.

According to Sterzel et al. [55], the shear modulus of Zn–Mn–Y quasicrystals is about 46 Gpa. According to Edagawa [56], Zhu and henley [57], the phonon–phason coupling coefficient of Mn–Ga–Al–Zn quasicrystals is -0.03μ and $K_2/K_1 \approx 0.6$, $K_1 = 0.3$ Gpa. Based on these experimental analyzes and predicted theories about quasicrystals, this paper gives the assumed material parameters as follows.

The Green's function obtained previously is based on the substrate which is transversely isotropic material. Considering the substrate of quasicrystal coating is usually made of steel materials, the constitutive relationship of transversely isotropic material needs be degenerated to apply to steel substrate. It is not accurate for the cooperation constants between quasicrystals and steel materials which still need to be further confirmed by the experiment. The material parameters of steel are presented as follows.

The following non-dimensional components are used in the figures:

$$c_m = \frac{c_{1m}}{c_{33}}\,(m = 1, 2, 3)\,, \quad c_4 = \frac{c_{44}}{c_{33}}, \quad c_6 = \frac{c_{66}}{c_{33}},$$

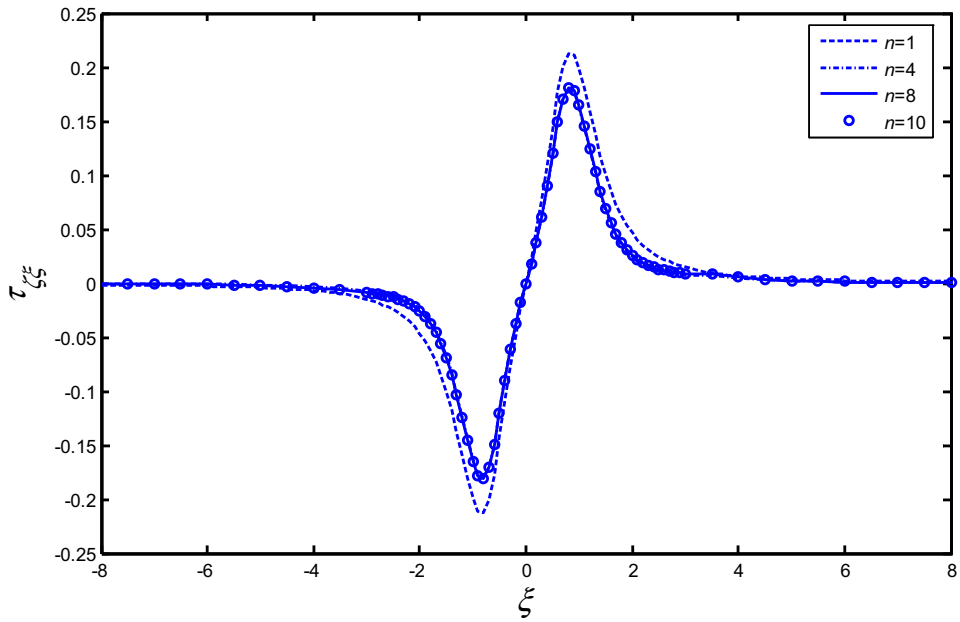

FIG. 2. Non-dimensional Green's stress $\tau_{\xi\zeta}$ along the interface $z = 0$ under the point force

$$K_{nn} = \frac{K_n}{c_{33}}(n = 1, 2, r, z), \quad R_{nn} = \frac{R_n}{c_{33}}(n = 1, 2, 3),$$
$$\tau_{kl} = \frac{\tau_{ij}}{c_{33}}, \quad \sigma_k = \frac{\sigma_i}{c_{33}}(i, j = r, \phi, z;\ k, l = \xi, \varsigma, \zeta),$$
$$\xi = \frac{r}{h}, \quad \zeta = \frac{z}{h}, \quad \varsigma = \frac{\phi}{h}, \tag{50}$$

where h is the coating thickness layer, and the normal point force is

$$P_z = -c_{33}h_0^2. \tag{51}$$

4.1. Computational accuracy

The following Scarborough criterion is used to estimate the accuracy of above solution:

$$|\varepsilon_{\mathrm{a}}| \langle \varepsilon_{\mathrm{s}}, \tag{52}$$

where ε_a is the relative percentage error and $\varepsilon_{\mathrm{s}} = \left(0.5 \times 10^{2-m}\right)\%$ is the tolerance of relative percentage error. This criterion can keep at least that the first m significant digits are correct.

Consider that the coating–substrate system is composed of 1D hexagonal quasicrystals and isotropic material. The figures of $\tau_{\xi\zeta}$ along the interface $z = 0$ for different iterations n are plotted in Fig. 2.

As the value of n changes, there is no significant change about $\tau_{\xi\zeta}$ in the graph, indicating that the numerical algorithm is convergent and accurate. When $n = 10$, the relative percentage error is only 0.01. Usually, the requirement for the computational accuracy in engineering is two significant digits. Therefore, the calculation results are also valuable.

Since the force acting on the coating is dimensionless unit force, the output of stress and displacement is very small in numerical value. In order to see its change rule more clearly, the value of the image

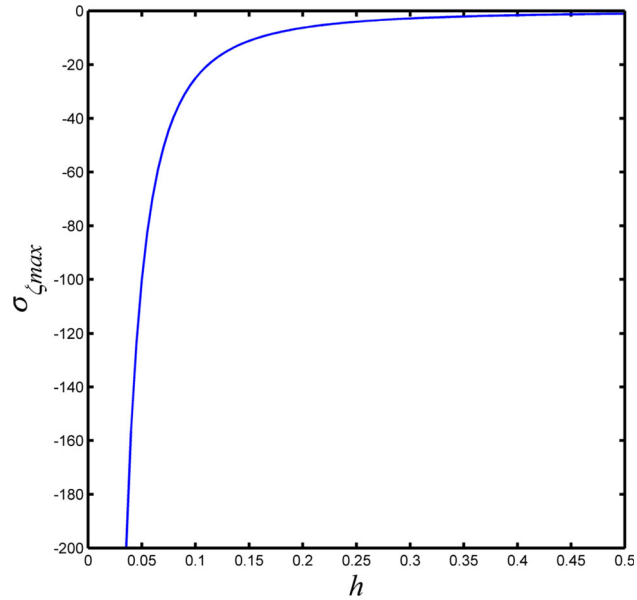

FIG. 3. Influence of the coating thickness on the distribution of the maximum σ_ζ along the interface under the same point force

is enlarged. The integral density of all contours is 0.02, which can not only ensure the accuracy of the output results, but also make the contour continuous and smooth.

4.2. The influence of the coating thickness and the magnitude of forces on the interface

In this section, the contours of the influence of the coating thickness and the magnitude of forces on the interface are given to present the use of this mathematical method in quantitative analysis. The contours are plotted in Figs. 3, 4 and 5, and some conclusions from the contours follow behind.

Some observations and suggestions from these contours are illustrated below:

1. Figure 3 and 4 present that the thinner the coating thickness, the more dramatic changes in the stress elastic field along the interface under the same point force. If the coating is thickened continuously, the stress increase is no longer significant. The stress distribution of other stress components, like σ_ξ, σ_ς, H_ζ, H_ξ, are similar to σ_ζ, $\tau_{\zeta\xi}$.
2. When $h \leq 0.216$, the curvature of the stress curve in Fig. 3 is greater than 50, which means at this time if the thickness decreases a little, the stress will increase a lot. The same change rule occurs in Fig. 4 when $h \leq 0.193$. This phenomenon indicates that, when the quasicrystals are used as coating material, the properties are very sensitive to its thickness and both the shear and normal stress should be considered simultaneously.
3. Figs. 3 and 4 present that the shear stress and normal stress of coating are closely related to the h.

From Eq. (51), we get

$$P_z \propto h_0^2, \tag{53}$$

then

$$H = h/h_0, \tag{54}$$

where h is the real thickness of the coating, H is the non-dimensional thickness of the coating and h_0 is the standard thickness of the coating.

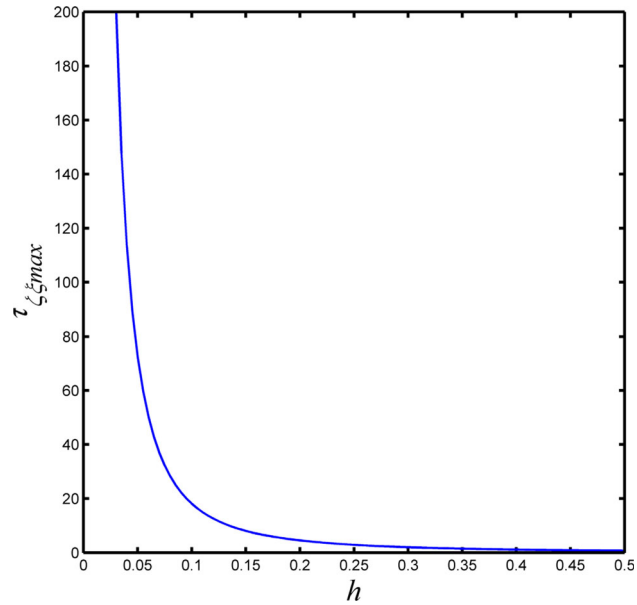

FIG. 4. Influence of the coating thickness on the distribution of the maximum $\tau_{\zeta\xi}$ along the interface under the same point force

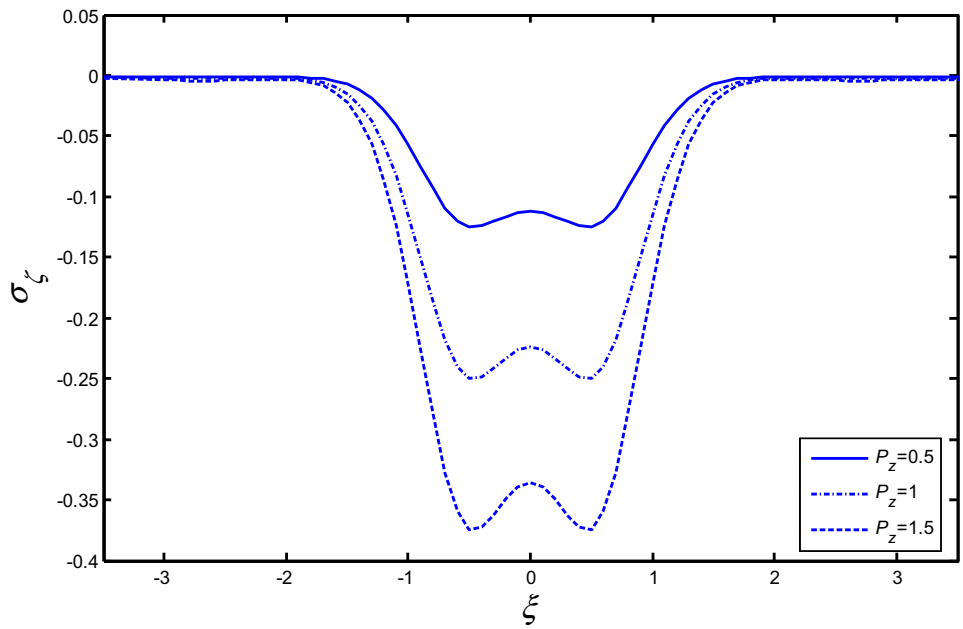

FIG. 5. Influence of the force on the distribution of $\sigma_\zeta \times 10^2$ along the interface under the same coating thickness

From Eqs. (53) and (54), it can be known that P_z at this time is affected by the real thickness h, because H is constant value. But in fact, what needs to be discussed about the influence of thickness is working under the constant tangential point force P_z. Therefore, when the input data of real thickness increased,

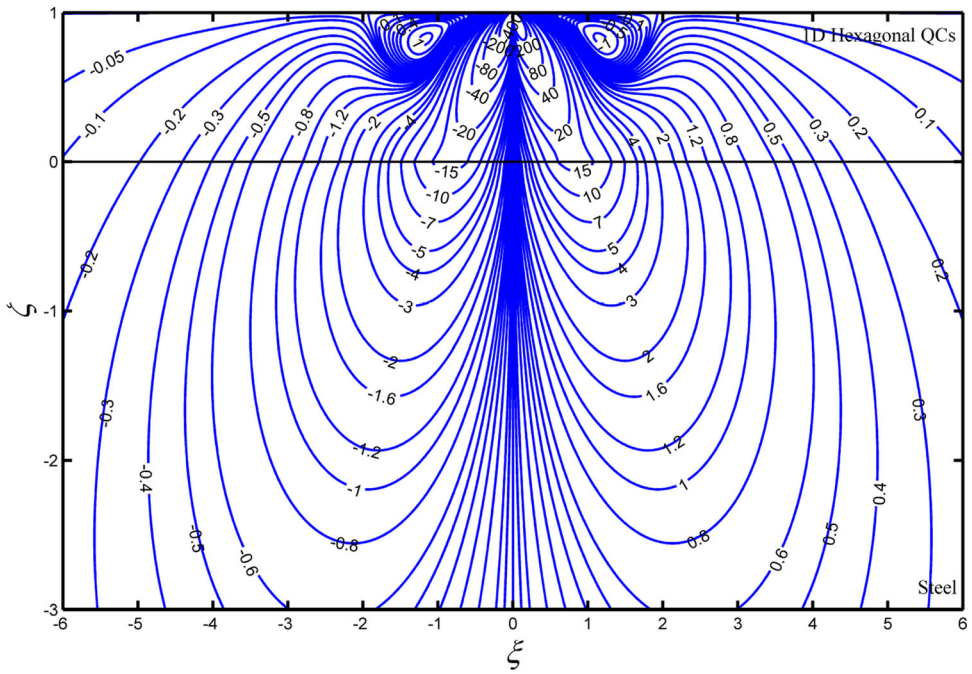

FIG. 6. Contour of non-dimensional Green's stress $\tau_{\zeta\xi} \times 10^2$ in phonon field under the point force

the output results of stress components should be quantitatively reduced. Finally, the relationship between the stress components and the thickness can be obtained by Dimensional Method:

$$\sigma_z \propto \frac{1}{h^2}, \quad \tau_{zr} \propto \frac{1}{h^2}. \tag{55}$$

5. Contours of stress components in the phonon and phason fields at the origin under the point force

In this section, based on the obtained Green's function solution and MATLAB programming, the contours of non-dimensional stress components $\tau_{\zeta\xi}$, σ_ξ, σ_ς, σ_ζ in phonon field, H_ξ, H_ζ in phason field and phason displacements w are given to present the application of this mathematical method in quantitative analysis. The contours are plotted in Figs. 6, 7, 8, 9, 10, 11 and 12, and some conclusions from the contours follow behind.

Some observations and suggestions from these contours are illustrated below:

1. It is observed that all stress components tend to zero in the far field and are tightly gathered around the point where the normal point force is acted. It can be found that there exists relatively large stresses and stress gradients in coating layer, especially near the point loading. This phenomenon means that most of the elastic energy is bounded in the coating layer and tells us a high strength level is needed for a good coating material.
2. The contours of the stress $\tau_{\zeta\xi}$ and σ_ζ are continuous at the interface in Figs. 6 and 9. This is coincident to the interface compatibility conditions. The gradient of stress is discontinuous when they travel across the interface. This phenomenon is caused by the difference of the material properties between coating and substrate, and this is more obvious in the contours of quasicrystals and non-quasicrystals.

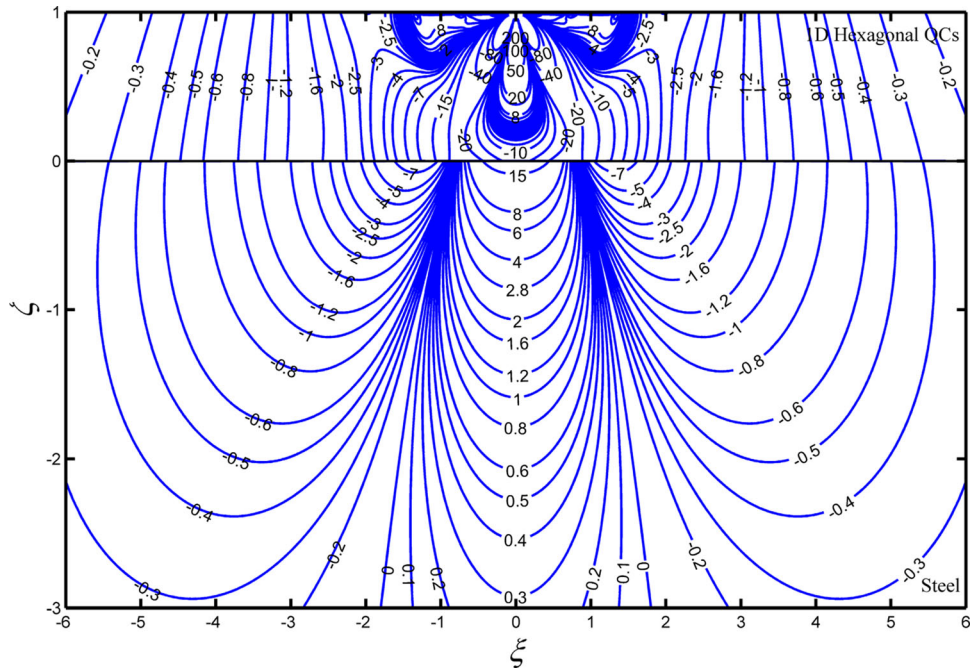

FIG. 7. Contour of non-dimensional Green's stress $\sigma_\xi \times 10^2$ in phonon field under the point force

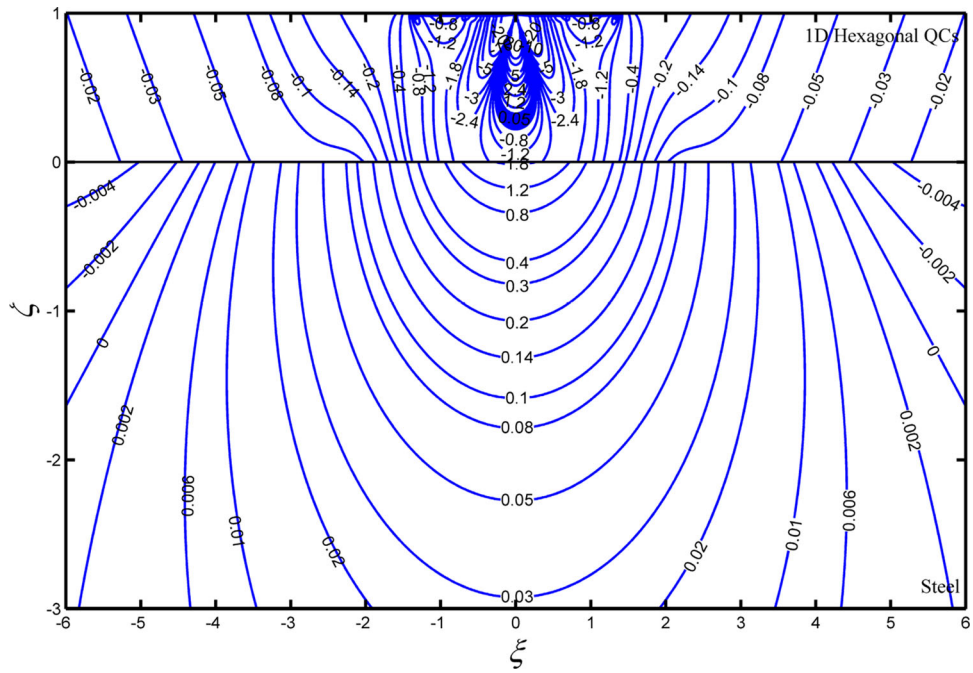

FIG. 8. Contour of non-dimensional Green's stress $\sigma_\varsigma \times 10$ in phonon field under the point force

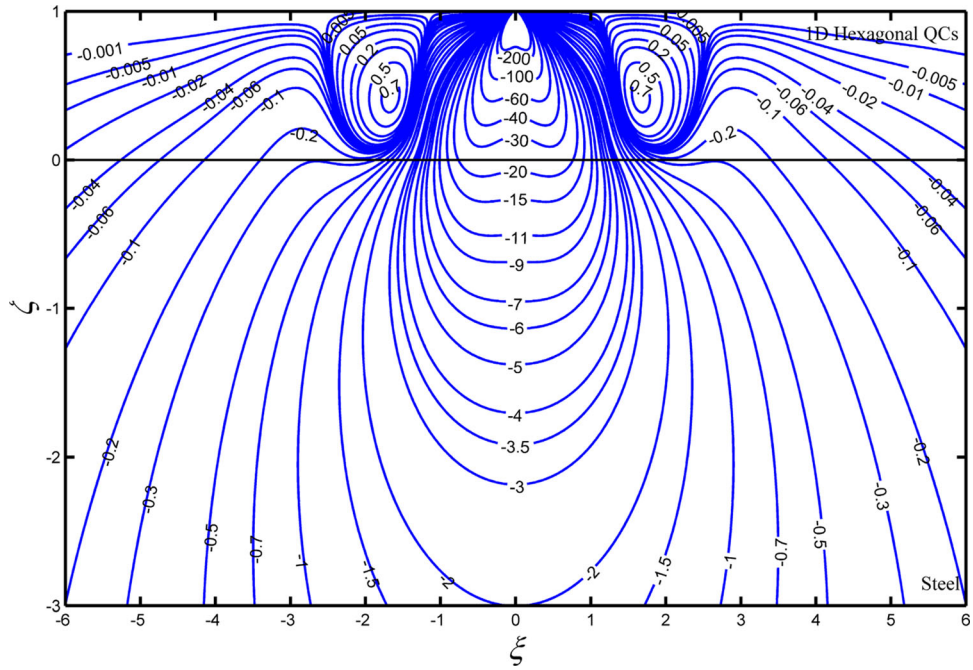

FIG. 9. Contour of non-dimensional Green's stress $\sigma_\zeta \times 10^2$ in phonon field under the point force

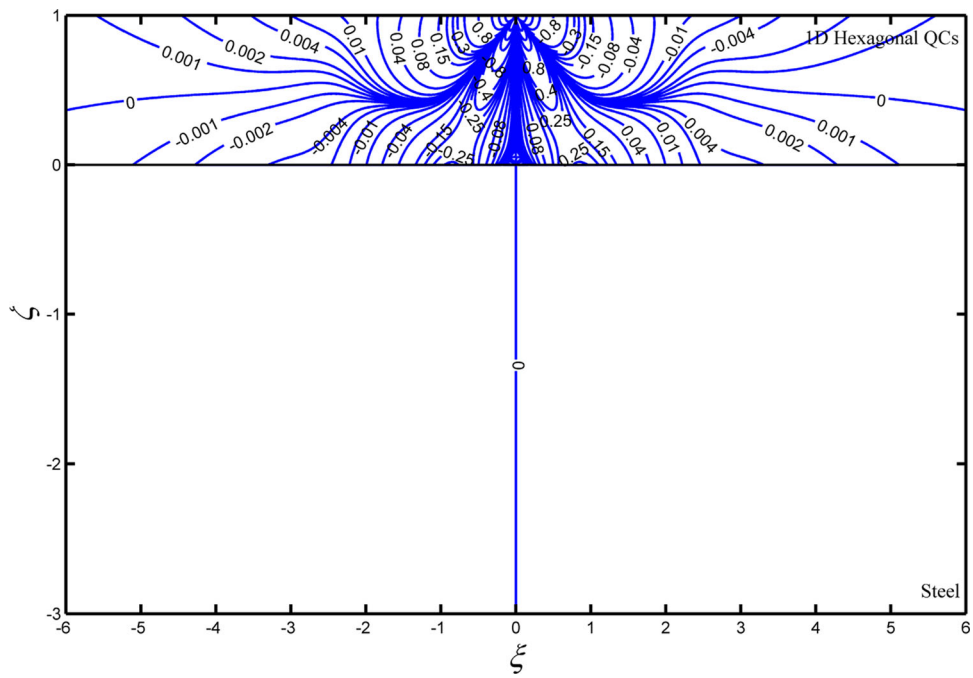

FIG. 10. Contour of non-dimensional Green's stress $H_\xi \times 10^2$ in phason field under the point force

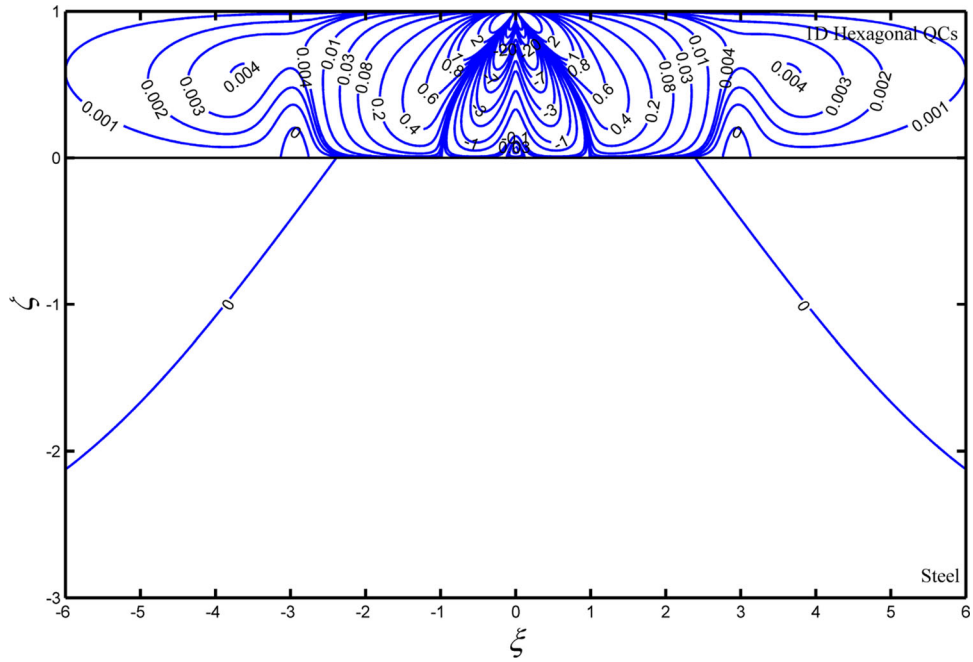

FIG. 11. Contour of non-dimensional Green's stress $H_\zeta \times 10^3$ in phason field under the point force

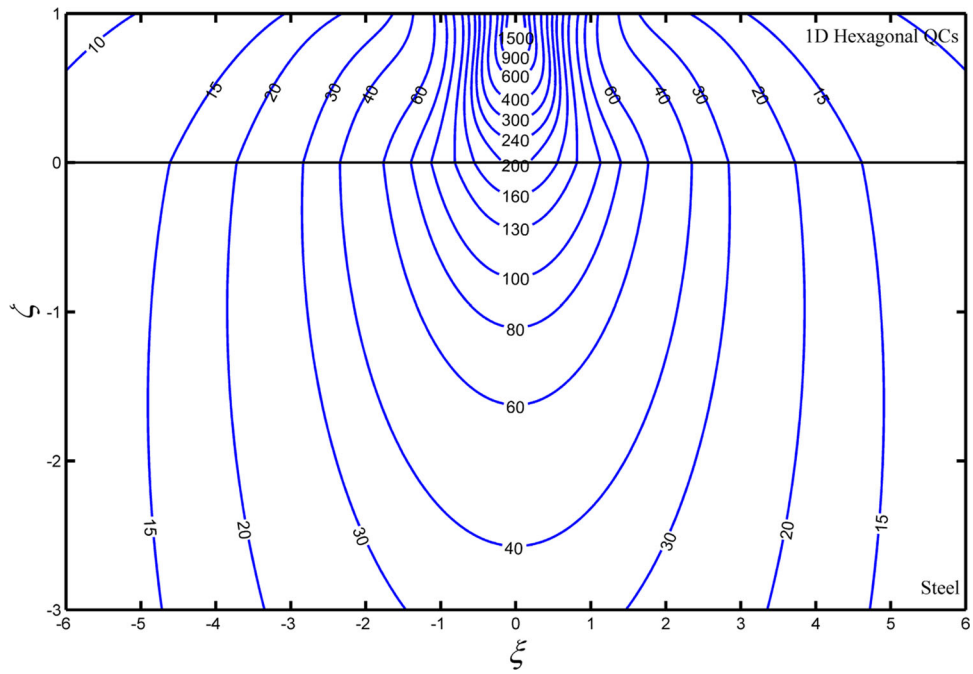

FIG. 12. Contour of non-dimensional Green's phason displacements $w \times 10^2$ under the point force

3. It can be found that there are several zero contours for the stress components where stress gradient changes largely. This dramatic change of stress field can result in the convergence of mechanical energy, and the micro-cracks would appear due to the generation of energy. In particular, the zero stress contours in Figs. 7, 8, 9, 10 and 11 which are normal stress components are more than that in Fig. 6 which are shear stress, leading to the energy convergence effect in the former more serious than the latter, which is more easily to be the failure of quasicrystal coating.
4. After comparison, the zero contours of stress usually occur in the vicinity of the point force below or on both sides of the ζ-axis. However, it should be noted that these areas prone to damage are not only confined to the coating. In Figs. 6, 7 and 8, a wide range of stress mutation also occurs in the substrate.
5. It can be known that the normal and shear stresses at the interface may lead to tension and shear delamination, respectively. The normal stress at the interface is negative under the normal point force. Figure 6 presents that the maximum shear stress appears at the interface near the ζ-axis.
6. Since the stresses in Figs. 6 and 10 are discontinuous across the ζ-axis, this interfacial effect can cause the opposite stress state on both sides of the ζ-axis. The opposite stress states are the main reason of cracks appearing at the symmetry plane, and the accumulation and expansion of cracks can lead to interface delamination. Therefore, in the design of quasicrystal coating, this dangerous stress state should be avoided as much as possible.
7. It can be found that there are only a few zero contours in the substrate about the phason stress component H_ζ, H_ξ, which is caused by relatively small cooperation constants K_r and K_z. The phenomenon observed in Figs. 10 and 11 presents that relatively large phason stress component appears in coating layer, especially near the point loading. But the phason stress gradient is much smaller than phonon's.
8. Figure 12 presents that the contours of the non-dimensional Green's phason displacements w under the point force P_z. The phason displacements w is continuous at the interface $z = 0$. This is coincident to the interface compatibility conditions.

By observing, the value of these stress components is much smaller relative to the external force, indicating that quasicrystals own well-elastic properties and have a strong rigidity and stability compared to other materials. With the contours of these stress components, the interaction between the phonon–phason coupling field of the coating and the elastic field of the substrate when acted by force field can be observed directly, which can be used to determine the location where the physical model is prone to damage, so as to provide a theoretical basis for the quasicrystal used as new coating material.

6. Contours of stress components in the phonon and phason fields under the different distributed forces

The Green's function obtained previously is the analytic solution of the whole field under the unit concentrated force. In order to obtain the solution under different distributed forces (cone force, cylindrical force, uniform force, ellipsoid force, uneven force etc.), the functions of distributed force need to be introduced and the matrix of the Green's function solution should be superimposed appropriately.

The function of ellipsoidal distribution is:

$$\sigma_z(r,\phi) = -\frac{3P_z}{2\pi ab}\sqrt{1-\frac{r^2\cos^2\phi}{a^2}-\frac{r^2\sin^2\phi}{b^2}}. \tag{56}$$

The function of conic distribution is:

$$\sigma_z(r,\phi) = -\frac{P_z}{\pi a^2}\cosh^{-1}\left(\frac{a}{r}\right). \tag{57}$$

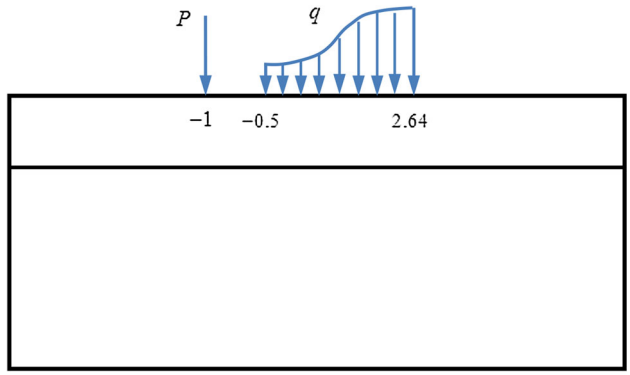

FIG. 13. Loading diagram of the uneven distributed force

The function of cylindrical distribution is:

$$\sigma_z(r,\phi) = -\frac{P_z}{2\pi a}\left(a^2 - r^2\right)^{-1/2}. \tag{58}$$

The loading diagram of the uneven distributed force is shown in Fig. 13, and the sine function of the distributed force is:

$$\sigma_z(r) = P_z(\sin(r - 1.07) + 2). \tag{59}$$

In this way, the analytical solution under the distributed forces, without any increase in the calculation amount, will be obtained through the combination of MATLAB programming skills and the Green's function matrix. This method can be used to simulate the solutions of quasicrystals quickly when working in different conditions, which provides a detailed theoretical basis for the industrial application of 1D hexagonal quasicrystals.

The contours of non-dimensional Green's stress components σ_ζ and $\tau_{\zeta\xi}$ under the different distributed forces are given to present the application of this mathematical method in quantitative analysis. The contours are plotted in Figs. 14 ,15, 16, 17, 18, 19, 20, 21, 22 and 23 and some conclusions follow behind.

Some observations and suggestions from these contours are illustrated below:

1. The contours of the distributed force have the same distribution as the point force. The stress components are continuous at the interface, which is consistent with the interface continuity condition. The larger stress is mainly distributed in the coating. Where the stress gradient is large, the elastic energy is concentrated. Therefore, these areas should be taken into account in the processing.
2. In all of the figures above, the larger stress is mainly distributed in the contact area, and the gradient is relatively gentle. The smaller stress is distributed at the edge of the contact area, however, resulting in a sharp increase in stress gradient. This is also the main cause of fracture at the boundary.
3. A stress mutation occurs at the contact area's boundary in both the cylindrical and uniform external forces, whereas the same area is relatively smooth in both the ellipsoidal and conical.
4. In Figs. 18 and 19, the stress is concentrated on the cone point and the cone contact area, and the stress gradient changes dramatically below the cone point in the coating. On the contrary, in Figs. 20 and 21, the large gradient occurs at the cylindrical edge.
5. By contrasting those stress contours, the characteristics of cylindrical distribution is same as the uniform force's, and the distribution of the cone is a combination of the point force and the ellipsoidal force.
6. Figures 22 and 23 show that the stress field inside the coating and the substrate change sharply and become more complicated when the outer surface is subjected to an uneven distributed external load. A large number of 0 contours make the structure of the quasicrystal coating more unstable,

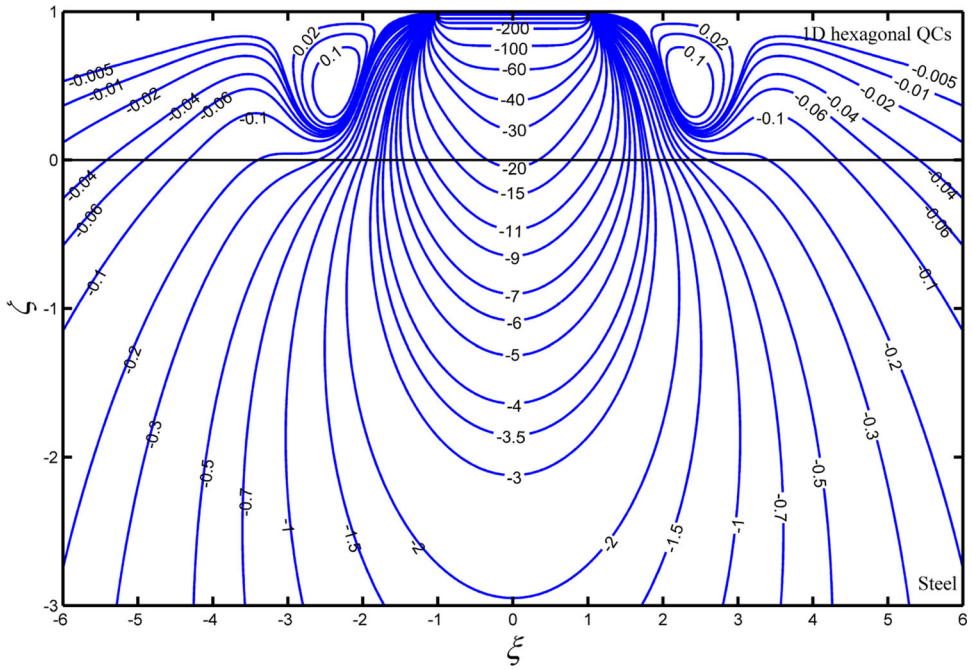

FIG. 14. Contour of non-dimensional Green's stress $\sigma_\zeta \times 10^2$ under the uniform force

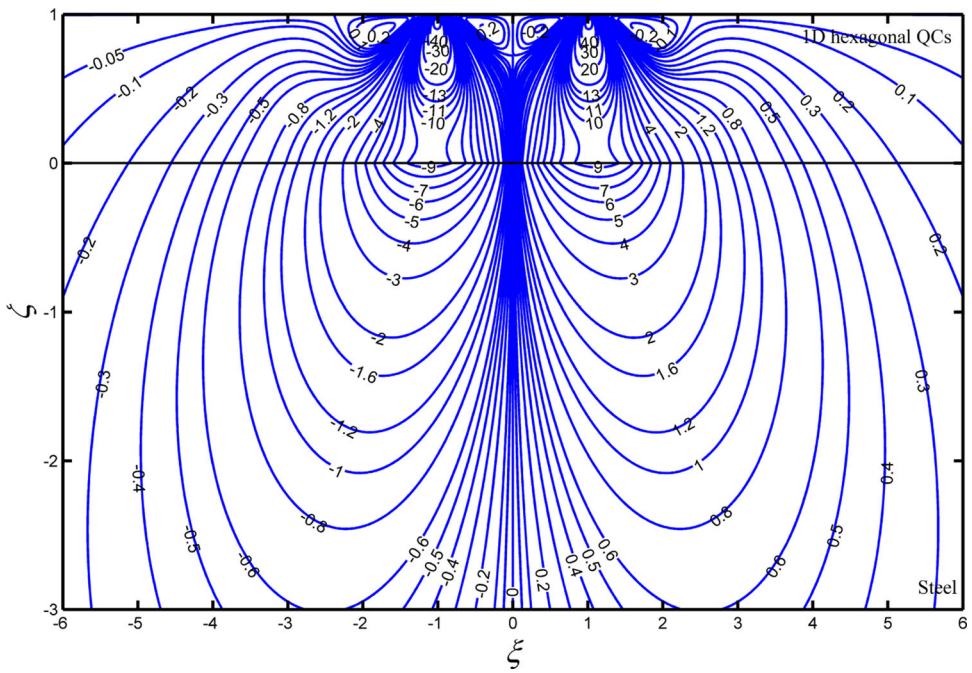

FIG. 15. Contour of non-dimensional Green's stress $\tau_{\zeta\xi} \times 10^2$ under the uniform force

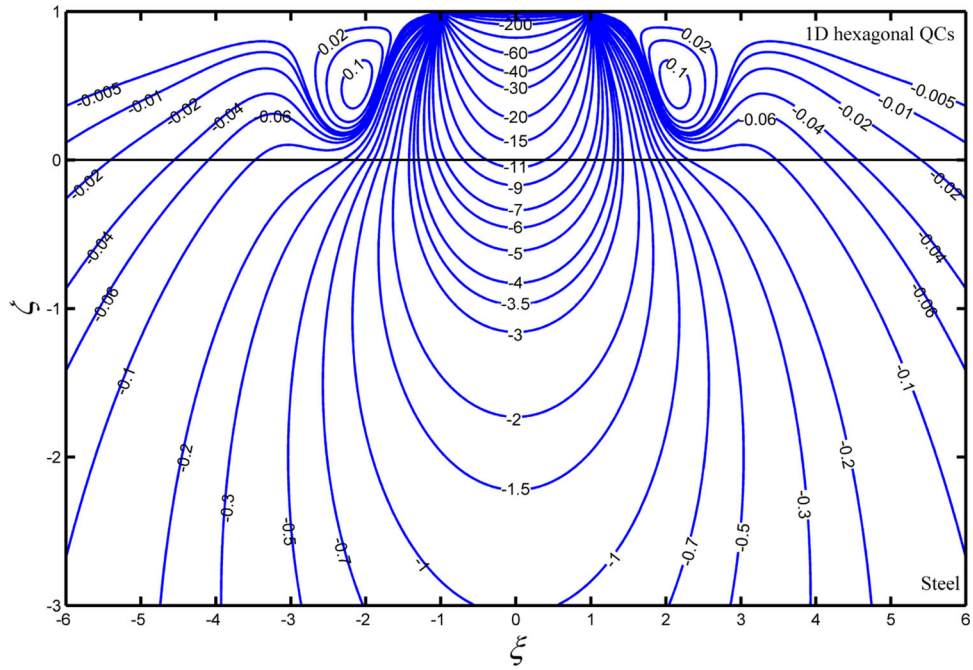

FIG. 16. Contour of non-dimensional Green's stress $\sigma_\zeta \times 10^2$ under the ellipsoidal force

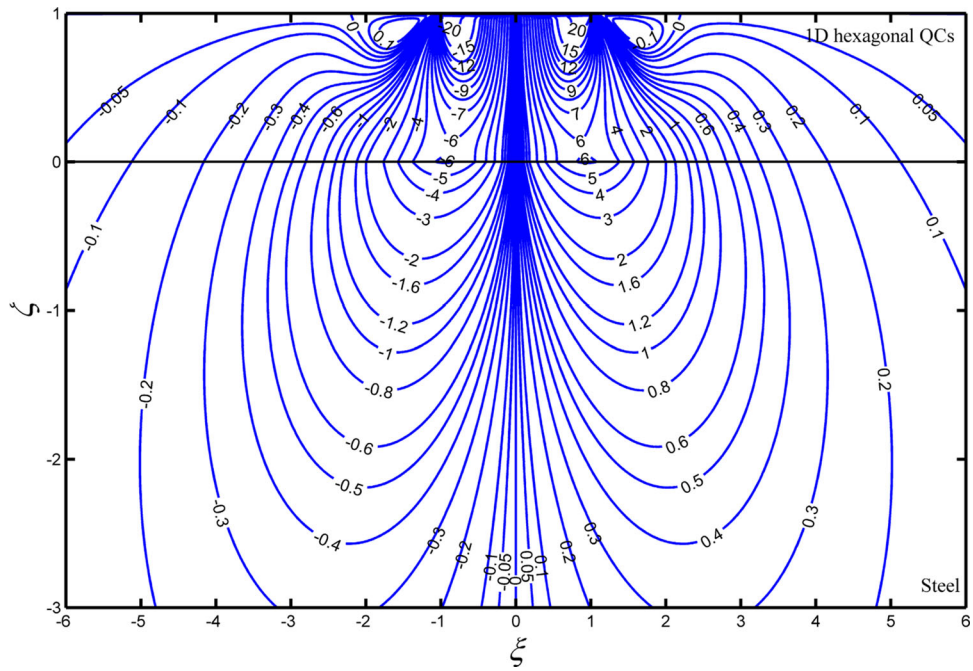

FIG. 17. Contour of non-dimensional Green's stress $\tau_{\zeta\xi} \times 10^2$ under the ellipsoidal force

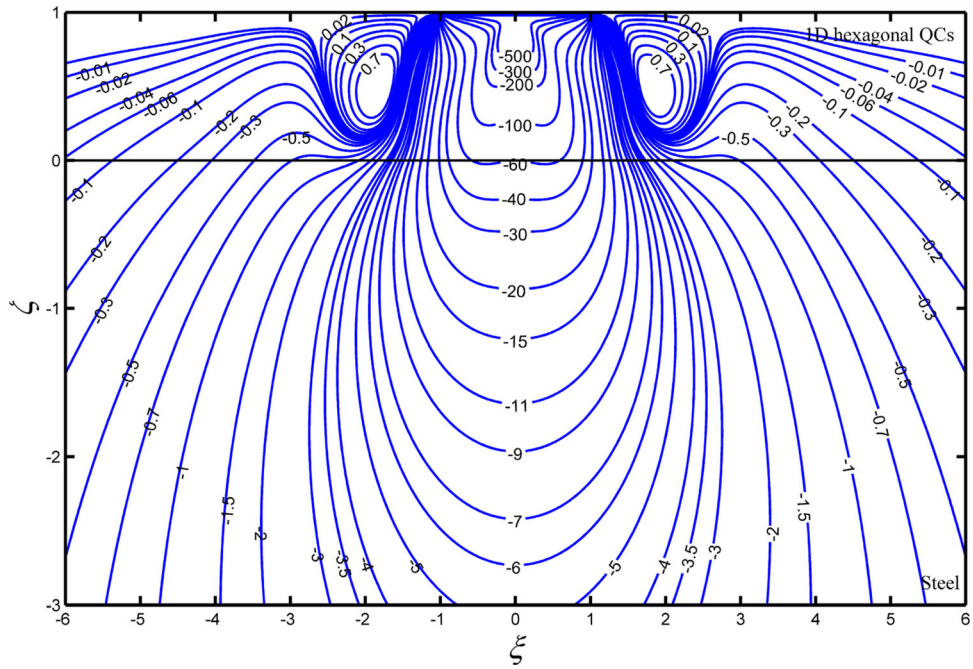

FIG. 18. Contour of non-dimensional Green's stress $\sigma_\zeta \times 10^2$ under the conical force

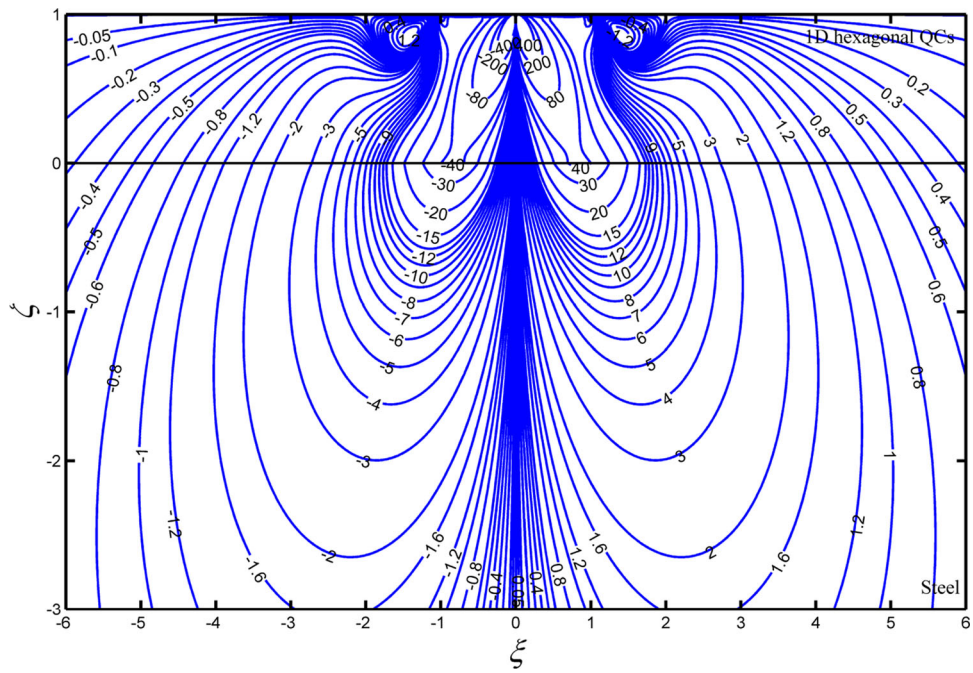

FIG. 19. Contour of non-dimensional Green's stress $\tau_{\zeta\xi} \times 10^2$ under the conical force

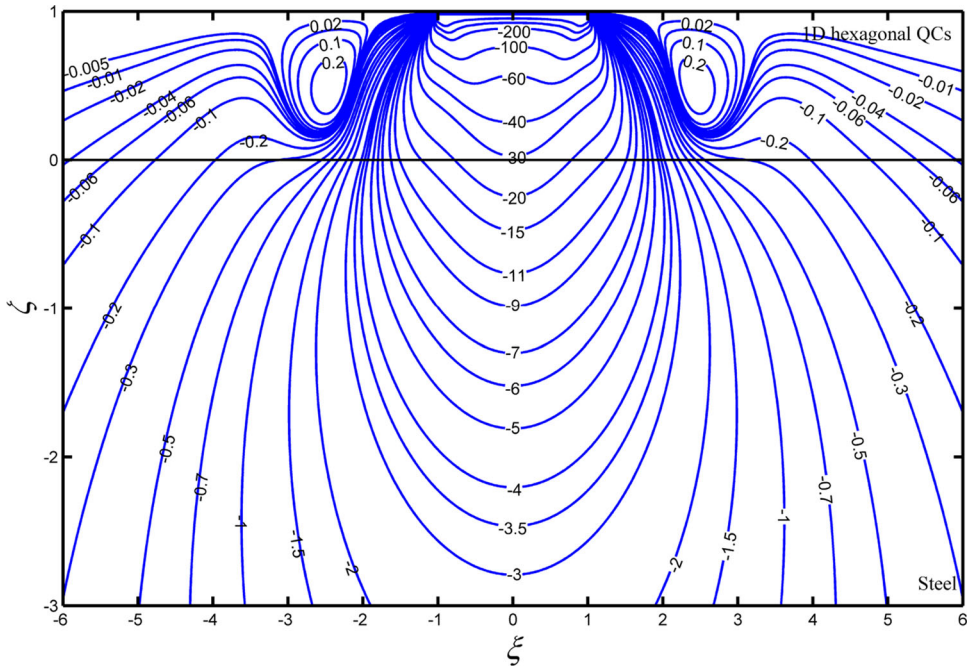

FIG. 20. Contour of non-dimensional Green's stress $\sigma_\zeta \times 10^2$ under the cylindrical force

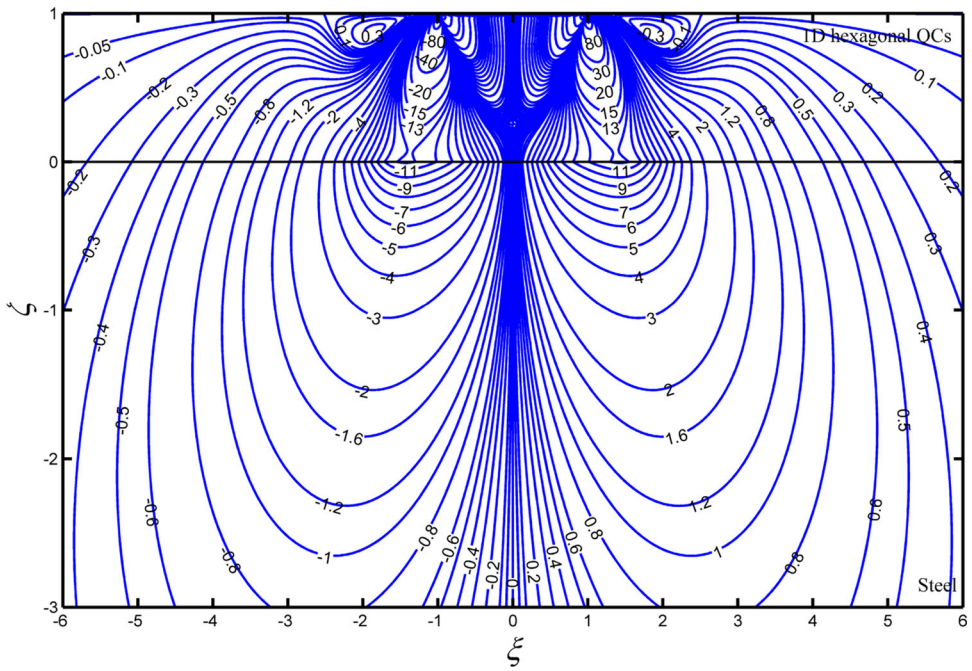

FIG. 21. Contour of non-dimensional Green's stress $\tau_{\zeta\xi} \times 10^2$ under the cylindrical force

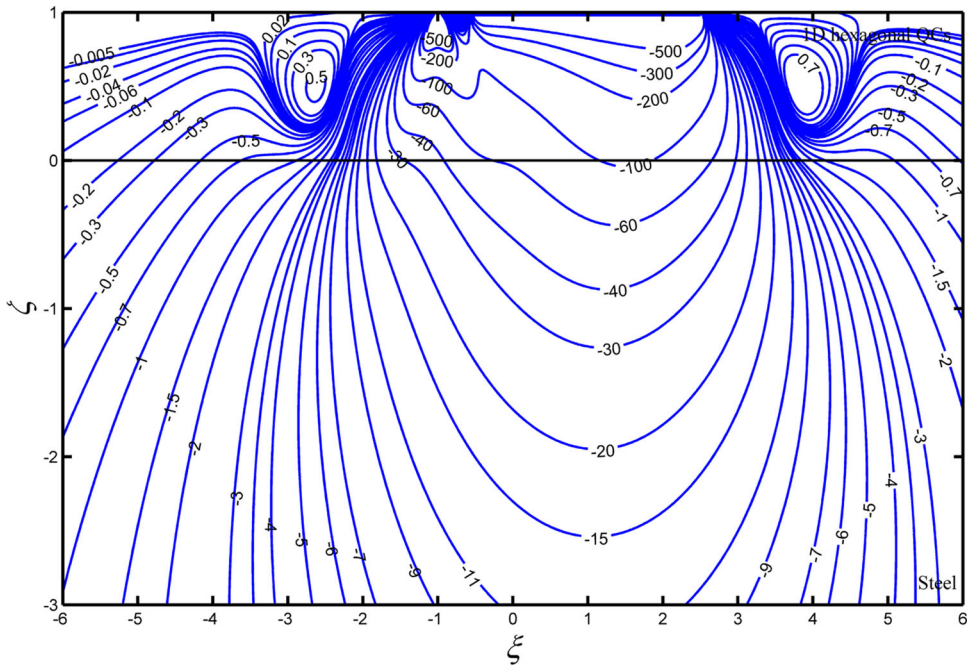

FIG. 22. Contour of non-dimensional Green's stress $\sigma_\zeta \times 10^2$ under the uneven distributed force

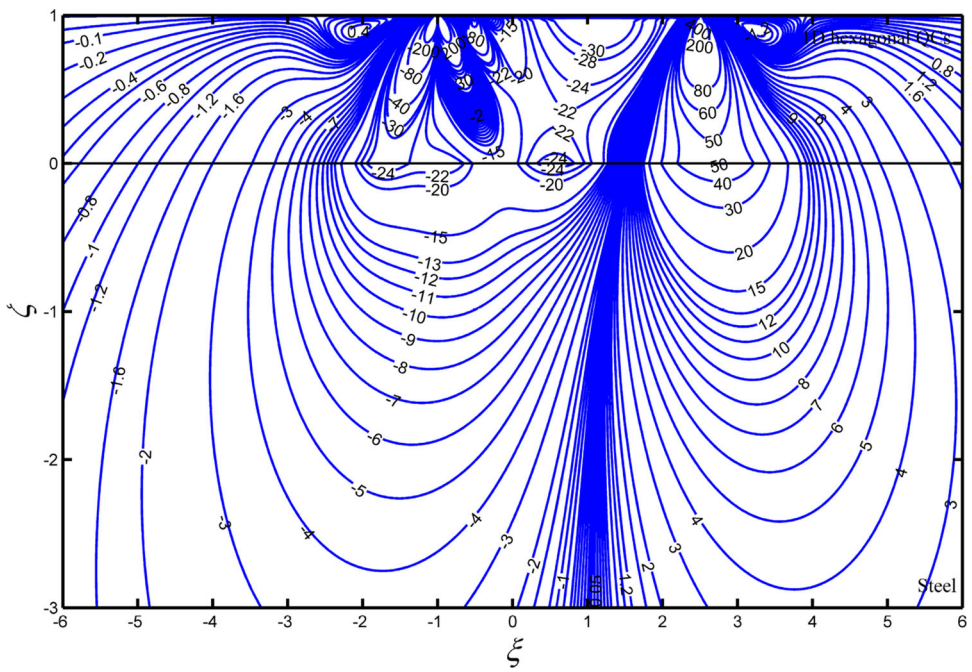

FIG. 23. Contour of non-dimensional Green's stress $\tau_{\zeta\xi} \times 10^2$ under the uneven distributed force

prone to delamination damage. Therefore, an accurate and efficient analytical method is particularly important for the application of quasicrystal coating, which is also the advantage of this paper.

With the knowledge obtained above, it can be found that the stress distributions are multifarious under the different distributed forces. It is presented that the coupled field components under the distributed load are not singular and satisfy the surface boundary condition when the superposition principle are used, although all the coupled field components are singular under the point force. This means that the Green's function solution under the point load can be used to solve various engineering problems effectively. Thus, the coating thickness and material can be changed to adapt to various application requirements, so as to obtain a more ideal stress state.

7. Conclusions

The desired harmonic functions (in Eqs. 28, 29, 32, 33) of three-dimensional Green's function for 1D hexagonal quasicrystals used as coating material have been deduced. And the relationship between phonon–phason coupling field of 1D hexagonal quasicrystals and the elastic field of transversely isotropic materials are presented when the coating surface is acted by different forms of forces, which is widely used in engineering, especially in coating surfaces for engines, solar cells, nuclear fuel containers and heat converters. Based on the principle of superposition, the newly developed Green's solution of 1D hexagonal quasicrystals in coating contact space is explicitly presented in terms of elementary functions. The interactions among the force field and the phonon–phason coupling elastic field are also revealed. This Green's function is essential in the boundary element method as well as the study of cracks, defects and inclusions.

In addition, the Green's solutions under different distributed forces (cone force, cylindrical force, uniform force, ellipsoid force, uneven force, etc.) are obtained through the combination of MATLAB programming skills and the Green's function matrix. This method can be used to simulate the solutions of quasicrystals quickly when working in different conditions, which provides a detailed theoretical basis for the industrial application of 1D hexagonal quasicrystals.

Because the obtained solution is expressed in terms of elementary functions, it is convenient to use. Numerical examples show us that the interfacial debonding and coating tensile failure should be paid attention to during the analysis and design of the coating materials.

Funding

Funding was provided by National Natural Science Foundation of China (Grant No. 11572119).

References

[1] Shechtman, D., Blech, I., Gratias, D., Cahn, J.W.: Metallic Phason with Long-Range Orientational Order and No Translational Symmetry, vol. 53. Wiley, New York (2013)
[2] Fan, T.Y.: Mathematical Theory of Elasticity of Quasicrystals and Application. Springer, Berlin (2010)
[3] Bak, P.: Phenomenological theory of icosahedral incommensurate ("quasiperiodic") order in Mn–Al alloys. Phys. Rev. Lett. **54**(14), 1517 (1985)
[4] Bak, P.: Symmetry, stability, and elastic properties of icosahedral incommensurate crystals. Phys. Rev. B **32**(9), 5764–5772 (1985)
[5] Letoublon, A., De Boissieu, M., Boudard, M., Mancini, L., Gastaldi, J., Hennion, B., Caudron, R., Bellissent, R.: Phason elastic constants of the icosahedral AI–Pd–Mn phason derived from diffuse scattering measurements. Philos. Mag. Lett. **81**(4), 273–283 (2001)
[6] Francoual, S., Kaneko, Y., Boissieu, M.D.: Diffuse scattering and phason fluctuations in the Zn–Mg–Sc icosahedral quasicrystal and its Zn–Sc periodic approximant. Phys. Rev. Lett. **95**(10), 105503/1-4 (2005)

[7] Edagawa, K., So, G.Y.: Experimental evaluation of phonon–phason coupling in icosahedral quasicrystals. Philos. Mag. A **87**(1), 77–95 (2007)
[8] Chernikov, M.A., Ott, H.R.: Elastic moduli of a single quasicrystal of decagonal AI–Ni–Co: evidence for transverse elastic isotropy. Phys. Rev. Lett. **80**(2), 321–324 (1998)
[9] Jeong, H.C., Steinhardt, P.J.: Finite-temperature elasticity phason transition in decagonal quasicrystals. Phys. Rev. B Condens. Matter **48**(13), 9394–9403 (1993)
[10] Socolar, J.E.S.: Simple octagonal and dodecagonal quasicrystals. Phys. Rev. B **39**(15), 10519 (1989)
[11] Wang, X., Pan, E.: Analytical solutions for some defect problems in 1D hexagonal and 2D octagonal quasicrystals. Pramana **70**(5), 911–933 (2008)
[12] Guo, J., Yu, J., Xing, Y., Pan, E., Li, L.: Thermoelastic analysis of a two-dimensional decagonal quasicrystal with a conductive elliptic hole. Acta Mech. **227**(9), 2595–2607 (2016)
[13] Destainville, N., Mosseri, R., Bailly, F.: Configurational entropy of codimension-one tilings and directed membranes. J. Stat. Phys. **87**(3), 697–754 (1997)
[14] Torian, S.M., Mermin, N.D.: Mean-field theory of quasicrystalline order. Phys. Rev. Lett. **54**(14), 1524 (1985)
[15] Gao, Y., Zhao, Y.T., Zhao, B.S.: Boundary value problems of holomorphic vector functions in 1D quasicrystals. Phys. B Condens. Matter **394**, 56–61 (2007)
[16] Liu, G.T., Fan, T.Y., Guo, R.P.: Displacement function and simplifying of plane elasticity problems of two-dimensional quasicrystals with noncrystal rotational symmetry. Mech. Res. Commun. **30**(4), 335–344 (2003)
[17] Liu, G.T., Fan, T.Y., Guo, R.P.: Governing equations and general solutions of plane elasticity of one-dimensional quasicrystals. Int. J. Solids Struct. **41**(14), 3949–3959 (2004)
[18] Peng, Y.Z., Fan, T.Y.: Crack and indentation problems for one-dimensional hexagonal quasicrystals. Phys. Condens. Matter **21**(1), 39–44 (2001)
[19] Chen, W.Q., Ma, Y.L., Ding, H.J.: On three-dimensional elastic problems of one-dimensional hexagonal quasicrystal bodies. Mech. Res. Commun. **31**(6), 633–641 (2004)
[20] Wang, X.: The general solution of one-dimensional hexagonal quasicrystal. Mech. Res. Commun. **33**(14), 576–580 (2006)
[21] Gao, Y., Zhao, B.S.: A general treatment of three-dimensional elasticity of quasicrystals by an operator method. Phys. Status Solidi (B) **243**(15), 4007–4019 (2006)
[22] Gao, Y., Zhao, B.S.: General solutions of three-dimensional problems for two-dimensional quasicrystals. Appl. Math. Model. **33**(8), 3382–3391 (2009)
[23] Li, X.Y., Li, P.D.: Three-dimensional thermo-elastic general solutions of one-dimensional hexagonal quasi-crystal and fundamental solutions. Phys. Lett. A **376**(26–27), 2004–2009 (2012)
[24] Yang, L.Z., Zhang, L.L., Song, F., Gao, Y.: General solutions for three-dimensional thermoselasticity of two-dimensional hexagonal quasicrystals and an application. J. Therm. Stresses **37**(3), 363–379 (2014)
[25] De, P., Pelcovits, R.A.: Linear elasticity theory of pentagonal quasicrystals. Phys. Rev. B Condens. Matter **35**(16), 8609 (1987)
[26] Bachteler, J., Trebin, H.R.: Elastic Green's function of icosahedral quasicrystals. Eur. Phys. J. **4**(3), 299–306 (1998)
[27] Gao, Y., Xu, S.P., Zhao, B.S.: A theory of general solutions of 3D problems in 1D hexagonal quasicrystals. Phys. Scr. **77**(1), 015601 (2008)
[28] Li, P.D., Li, X.Y., Zheng, R.F.: Thermo-elastic Green's functions for an infinite bi-material of one-dimensional hexagonal quasicrystals. Phys. Lett. A **377**(8), 637–642 (2013)
[29] Li, X.Y., Deng, H.: On 2D Green's functions for 1 D hexagonal quasicrystals. Phys. B Condens. Matter **430**, 45–51 (2013)
[30] Li, X.Y., Li, P.D., Wu, T.H., Shi, M.X., Zhu, Z.W.: Three-dimensional fundamental solutions for one-dimensional hexagonal quasicrystal with piezo-electric effect. Phys. Lett. A **378**(10), 761–856 (2014)
[31] Li, X.Y., Wang, T., Zheng, R.F., Kang, G.Z.: Fundamental thereto-electro-elastic solutions for 1D hexagonal QC. J. Appl. Math. Mech. **95**(5), 457–468 (2015)
[32] Gao, Y., Ricoeur, A.: Three-dimensional Green's functions for two-dimensional quasi-crystal bi materials. Proc. Math. Phys. Eng. Sci. **467**(2133), 2622–2642 (2011)
[33] Wang, T., Li, X.Y., Zhang, X., Muller, R.: Fundamental solutions in a half space of two-dimensional hexagonal QC and their applications. J. Appl. Phys. **117**, 154904 (2015)
[34] Markus, L., Eleni, A.: Fundamentals in generalized elasticity and dislocation theory of quasicrystals: Green tensor, dislocation key-formulas and dislocation loops. Philos. Mag. **94**(35), 4080–4101 (2014)
[35] Chen, J.J., Bull, S.J.: Modelling the limits of coating toughness in brittle coated systems. Thin Solid Films **517**, 3704–3711 (2009)
[36] Song, Z., Komvopoulos, K.: Delamination of an elastic film from an elastic-plastic substrate during adhesive contact loading and unloading. Int. J. Solids Struct. **50**(16–17), 2549–2560 (2013)
[37] Huang, X.Q., Pelegri, A.A.: Finite element analysis on nanoindentation with friction contact at the film/substrate interface. Compos. Sci. Technol. **67**(7–8), 1311–1319 (2007)

[38] Kouitat, N.R., Von, S.J.: Boundary element numerical modelling as a surface engineering tool: application to very thin coatings. Surf. Coat. Technol. **116–119**, 573–9 (1999)
[39] Kouitat, N.R., Niane, N.T., Stebut, J.V.: Three-dimensional vertical cracks ln coated specimens under sliding contact load with a spherical indenter: a numerical study using boundary element modeling. Surf. Coat. Technol. **200**, 894–7 (2005)
[40] Mal, A.K.: Guided waves in layered solids with interface zones. Int. J. Eng. Sci. **26**, 873–881 (1988)
[41] Mal, A.K.: Wave propagation in layered composite laminates under periodic surface loads. Wave Motion **10**, 257–266 (1988)
[42] Thomson, W.T.: Transmission of elastic waves through a stratified medium. J. Appl. Phys. **21**, 89–93 (1950)
[43] Haskell, A.: The dispersion of surface waves on a multilayered media. Bull. Seismol. Soc. Am. **43**, 17–34 (1953)
[44] Gilbert, F., Backus, G.: Propagator matrices in elastic wave and vibration problems. Geophys **31**, 326–332 (1966)
[45] Banerjee, P.K., Butterfield, R.: Boundary Element Methods in Engineering Science, pp. 35–71. Springer, Berlin (1981)
[46] Elliott, H.A.: Three-dimensional stress distributions in hexagonal aeolotropic crystals. Math. Proc. Cambr. Philos. Soc. **44**, 522–533 (1948)
[47] Willis, J.R.: The elastic interaction energy of dislocation loops ln anisotropic media. Q. J. Mech. Appl. Math. **18**, 419–433 (1965)
[48] Sveklo, V.A.: Concentrated force in a transversely isotropic half-space and in a composite space. J. Appl. Math. Mech. **33**, 532–537 (1969)
[49] Pan, Y.C., Chou, T.W.: Point force solution for an infinite transversely isotropic solid. J. Appl. Mech. ASME **43**(4), 514–515 (1976)
[50] Pan, E., Yuan, F.G.: Three-dimensional Green's functions in anisotropic biomaterials. Int. J. Solids Struct. **37**, 5329–5351 (2000)
[51] Pan, E.: Three-dimensional Green's functions in anisotropic elastic biomaterials with imperfect interfaces. J. Appl. Mech. ASME **70**, 180–190 (2003)
[52] Ding, H.J., Hou, P.F., Guo, F.L.: The elastic and electric fields for three-dimensional contact for transversely isotropic piezoelectric materials[J]. Int. J. Solids Struct. **37**(23), 3201–3229
[53] Wang, R.H., Yang, W.G., Hu, C.Z., Ding, D.H.: Point and space groups and elastic behaviour of one-dimensional quasicrystals. J. Phys. Condens. Matter **9**(11), 2411–2422 (1997)
[54] Ding, H.J., Cheng, W.Q., Zhang, L.C.: Elasticity of Transversely Isotropic Materials. Springer, Berlin (2006)
[55] Sterzel, R., Hinkel, C., Haas, A., Langsdorf, A., Bruls, G., Assmus, W.: Ultrasonic measurements on fci Zn–Mg–Y single crystals. Europhys. Lett. **49**(6), 742–747 (2007)
[56] Edagawa, K.: Phonon–phason coupling in a Mg–Ga–AI–Zn icosahedral. Philos. Lett. **85**(9), 455–462 (2005)
[57] Zhu, W.J., Henley, C.L.: Phonon-phason coupling in icosahedral quasicrystals. Europhys. Lett. **46**(6), 748–754 (1999)
[58] Wu, Y.F.: Indentation Analysis of Piezoelectric Materials and Quasicrystals. Zhejiang University, Hangzhou (2012)
[59] GB 50017-2003 Code for design of steel structures

Peng-Fei Hou, Bing-Jie Chen and Yang Zhang
State Key Laboratory of Advanced Design and Manufacturing for Vehicle Body
Hunan University
Changsha 410082
People's Republic of China

Peng-Fei Hou, Bing-Jie Chen and Yang Zhang
Department of Engineering Mechanics
Hunan University
Changsha 410082
People's Republic of China
e-mail: chenbingjie8@outlook.com

(Received: March 11, 2017; revised: July 25, 2017)